Master in Chemical Engineering

Development of a catalyst for accelerated hydrolytic degradation of PLA greenhouse twines

A Master's dissertation

of

Filipa Vieira Bastos e Ferraz Miranda

Developed within the course of dissertation

held in

Lankhorst Euronete Portugal, S.A. & Laboratory of Separation and Reaction Engineering and Laboratory of Catalysis and Materials, LSRE-LCM

Supervisor at FEUP: **Dr. Katarzyna Morawa Eblagon**

Co-supervisor at FEUP: **Prof. Dr. Manuel Fernando Ribeiro Pereira**

Supervisor at Lankhorst Euronete Portugal, S.A.: **Eng. Fernando Eblagon**

Departamento de Engenharia Química

July of 2018

CLASSIFIED DOCUMENT. USE ONLY FOR EVALUATION PURPOSES

"Paddle your way through it with head, heart and sinew"

Lord Robert Stephenson Smyth Baden-Powel of Gilwell, in "Rovering to Success" (1920)

Acknowledgments

To my supervisor Dr. Katarzyna, for being more than a supervisor during this project, for being a real committed partner, thank you. I also acknowledge to Professor Fernando and Eng. Fernando for all the empirical knowledge passed through these months that contributed to my academic development.

To the staff of Departamento de Engenharia Química who helped me with my analyses carried out of LCM: Luís Carlos Matos and Nuno Guerreiro with the particle size distribution analyses and Liliana Pereira with the TOC analyses.

To LCM researchers who were always available to help: Bruno, Carla, Lucília, Natália, Patrícia and Raquel, who helped me to analyse my TPD results.

To Lankhorst Euronete R&D department mainly to Dr. Manuel and Eng. Rui Bastos with their help with GPC analyses and tensile tests respectively.

To Dr. Daniela from CEMUP for the efficient SEM analysis including the help with the samples preparation and to Laboratório de Caracterização Química from Departamento de Engenharia de Polímeros da Universidade do Minho for the GPC analysis.

To Dr. Ana Arenillas de la Puente from Departamento de Processos Quimicos en Energia y Medioambiente for providing the F samples.

To Débora, Diogo, Miguel and Sofia for our moments as master thesis students in LCM laboratories.

To my daily girls - Ana Carolina, Filipa, Francisca, Ivete, Rita, Sara, Stéfanie – and to my daily boys – Bruno, Cláudio, Daniel, Emanuel, João, João and Tiago: you contributed more for this work that you can ever imagine. To Bruno and Joana and in you, all of the *ad aeternum* 38 best parts of me. Thank you is never going to be enough for all of you.

To Eng. Rafael, for all the moments when you were complaining about my scientific pride, cleaning my mess, taking care of the nitrogen and ethanol for me and sending me home to rest. I will be thankful to you forever for your contribution to my personal growth.

To my family (grandmother, grandfather, aunts, uncles, cousins and Ester) thank you for growing me up good enough to enrol and finish a MSc in the best *alma mater* I could ever asked for.

Mom, Dad and Tomás: finally, I have something to give you back a little of what you gave me during 23 years of a fulfilled life. Now, "*Mundo!*".

Abstract

Poly(lactic acid) twines are used in greenhouses to guide vegetables as they grow. By the end of the season the greenhouse needs to be cleaned up entirely. The PLA twines and the vegetables residues will be thrown away into a composting pile and both materials are expected to be degraded. This work intends to shorten the time of the hydrolytic degradation of PLA twines under composting conditions introducing catalysts in the fibres and thus reduce the composting days needed.

Four types of catalysts were chosen to provide a broader analysis of the problem: oxides, zeolites, clays and carbon catalysts. Several techniques such as: measurements of particle size distribution, textural characterization from B.E.T specific surface measurements, thermogravimetric analysis (TG) and scanning electron microscopy with energy dispersive spectroscopy (SEM/EDS) among others were performed to characterize the catalysts. Afterwards, the catalysts were included in the fibres by dry blending and extrusion obtaining PLA fibres with catalyst with the addition of a processing aid oligomer The effect of the oligomer was also studied. In addition, two polymers were applied as catalysts, in order to try and accelerate the hydrolytic decomposition of the PLA twines.

The prepared PLA fibres with the catalysts were tested under hydrolytic degradation with the fibres immersed in water. The pH and TOC of the reaction water were measured in order to establish the progress of the hydrolysis reaction of the fibres with the catalysts in comparison with the pristine PLA fibre. Scanning electron microscopy was performed to verify the morphologic changes before and after hydrolysis as well as the influence of the presence of the catalysts in the fibre. In addition, TG and tensile tests were performed in order to correlate the thermal stability and mechanical properties of the fibres to assess the advancement of the hydrolytic degradation of the polymer.

The experimental results indicated that the commercial clay C as shown by SEM/EDS was the best catalyst under the reaction conditions studied. It showed good catalytic activity (significantly shorten time of PLA degradation), no changes in thermal stability and improved fibre elongation. Last but not least, the clay is not expensive so it can be used on the larger scale in PLA twines production, it is generally recognized as safe and food contact approved.

Keywords (theme): Poly(lactic acid); Hydrolysis; PLA fibres; PLA twines; Catalysts

Declaration

I hereby declare, on my word of honour, that this work is original and that all non-original contributions were properly referenced with source identification.

Porto, July 2nd 2018

Index

List of Figures

List of Tables

Notation and Glossary

	Tenacity	gf·denier
	Flow	$cm^3 \cdot min^{-1}$
	Electron beam intensity	eV
	Particle size	µm
	Denier (can be abbreviated as “den”)	$1g \cdot 9000\ m^{-1}$
μ	Viscosity	Pa.s
$dV(d)$	Pore distribution	$cm^3 \cdot nm^{-1} \cdot g^{-1}$
f	Shear rate; ball-milling frequency	s^{-1}
l	Gauge	mm
m	Weight	g
M_n	Number average molecular weight	$g \cdot mol^{-1}$; Da
M_W	Weight average molecular weight	$g \cdot mol^{-1}$; Da
P	Pressure	Pa; psi; atm
P_0	Saturation pressure	Pa
R_D	Down ratio	
RH	Relative humidity	%
R_S; V_S	Stretch ratio	
S_{BET}	Specific surface area calculated by B.E.T. method	$m^2 \cdot g_{cat}^{-1}$
t	Time	s
T	Temperature	ºC; K
T_f	Filament titre entering the stretch	den
T_g	Glass transition temperature	ºC
T_m	Melting temperature	ºC
T_S	Filament titre exiting the stretch	den
v	Speed	$m \cdot s^{-1}$
V	Pore volume	$cm^3 \cdot g_{cat}^{-1}$
V_f	Spin rate	s^{-1}
V_L	Peripheral speed	$m \cdot s^{-1}$
wt	Weight percentage	%

Greek letters

ε	Elongation	%
Δ	Variations	%
λ	Wavelength	cm^{-1}

Indexes

Micro	Micropores
Meso	Mesopores
pzc	Point zero charge

List of Acronyms

B.E.T.	Brunanuer-Emmett-Teller
C	C Clay
C	Thermoregulated filament heating system
CA	Citric Acid
D	Carbon Black

DFT	Density Functional Theory
DI	Distillate water
DSC	Differential Scanning Calorimetry
EA	Elemental Analysis
EDS	Energy Dispersive Spectroscopy
F	Carbon F
FT-IR	Fourier-Transform Infra-Red Spectroscopy
GPC	Gel Permeation Chromatography
H	Rotating role
I	I Clay
J	J Clay
K	K Clay
L	Rotating role
LSRE-LCM	Laboratory of Separation and Reaction Engineering and Laboratory of Catalysis and Materials
n.d.	Non determined
PET	Polyethylene terephthalate
PIDS	Polarization Intensity Differential Scattering
PLA	Poly(lactic acid)
Polymer_A	Polymer A
Polymer_B	Polymer B
PP	Polypropylene
Process_Aid	Processing Aid
PS	Polystyrene
s.d.	Standard Deviation
SEM	Scanning Electron Microscopy
STP	Standard Temperature and Pressure
T	Tensioning device
TGA	Thermogravimetric Analysis
TOC	Total Organic Carbon
TPD	Temperature Programmed Desorption
US	Ultra-sonicated

1 Introduction

1.1 Background and presentation of the work

This main goal of this work is to reduce the time that is needed for the hydrolytic degradation of poly(lactic acid) (PLA) twines in composting conditions. In this work, selected catalysts with varied surface chemistry, chemical composition and structure will be characterized and then introduced in the fibres. The effect of the catalyst presence in the fibre was tested under hydrolytic degradation conditions. The best performing fibres (with the shortest degradation time) can be in the future transformed into twines supporting tomato plants in the greenhouses.

1.2 Presentation of the company

This master thesis was done in collaboration with Lankhorst Euronete Portugal, S.A. installations in Maia.

The company first started in 1803 as "Lankhorst Touwfabrieken" in Sneek, the Netherlands manufacturing ropes and netting [1]. In 1964, Euronete Ltd was founded in Matosinhos, Portugal by Captain Gramaxo [2]. In 1998, the Lankhorst Euronete group BV was created as a result of both companies' merger. By the year of 2012, WireCo. World Group, headquartered in Kansas City, USA, acquired Royal Lankhorst Euronete group BV. [3].

The group works actively within six diverse divisions: Maritime & Offshore Rope Division, Yarn Division, Pure Composites Division, Euronete Fishing Division, Engineered Products Division and Yachting Division. The Yarns Division is responsible for the development, production and commercialization of technical and industrial yarns used for agriculture, artificial grass, fences, geo-textiles and other industrial markets.

1.3 Contributions of the Work

PLA twines are used in greenhouses to guide vegetables as they grow, mainly tomatoes. However, by the end of the season, the greenhouse has to be cleaned entirely. The PLA twines and the vegetables residues are thrown into a composting pile and both materials are expected

to be degraded as fast as possible unlike the classic polypropylene (PP) fibres that cause a large amount of trash in the landfill.

Pieces of PLA twines are normally found at the end of the industrial composting cycle which increases the turnover time for the compost produced from this waste stream. Hence, this work intends to shorten the time of the hydrolytic degradation of PLA twines under composting conditions introducing catalysts in the fibres and thus reduce the composting days needed. As a result, the process turns more environmental friendly and more economical for the growers, who either end up paying less for the composting process or the composted product. The desired catalysts cannot influence the mechanical properties of the PLA fibres, they should be cost effective and ideally be food contact approved.

1.4 Organization of the thesis

Chapter 2 describes the Context and State of Art where the most important aspects about poly(lactic acid) (PLA) including properties, production conditions and most relevant applications are presented. The main characteristics of the catalysts which will be incorporated in the fibres are also described.

Chapter 3 describes the materials and methods used in this project including the details about the catalysts' functionalization methods used and characterization techniques of the pristine PLA fibres and PLA with the catalysts.

Chapter 4 contains the discussion of the results obtained from the catalytic tests and catalysts characterisation techniques.

Chapter 5 includes the discussion of the project results and their conclusions in the light of the goals of the project.

In the chapter 6 the obtained work is evaluated as well as the limitations that were found during this project. Suggestions of the follow up work are made in this chapter.

The appendixes have several complementary and useful information, for example: reactions mechanisms (manufacturing processes and responsible microorganisms), catalysts characterization results, hydrolysis control test results and results from fibres analysis (gel permeation chromatography, thermogravimetry and tensile tests).

2 Context and State of the Art

2.1 Twines for growing vegetables and fruits in greenhouses

Twines are used to maximize the use of available space in greenhouses by guiding the plant to grow vertically. Due to the fact that the greenhouses have to be cleaned yearly in preparation for the new crops, a large volume of waste containing a mix of plastic (i.e. twines) and organic residues (i.e. plants) is created. For example, the production of tomato in The Netherlands is evaluated as 500 tons' $year^{-1}$ ha^{-1}. Per each ha, 300 kg of twine are used representing 50 tons of waste at the end of the year [4].

The quantity of plastic is between 5 to 8 times larger than the amount of green residues. In addition, the separation process of the greenhouse waste is a very complex and expensive process. After separation, the organic part of this waste can be compostable or can be used as substrate in biogas production. In turn, biogas can be collected and employed to produce electricity. On the other hand, the non-degradable plastic trash ends up in landfill [4], where it stays for many years, contaminating water, soil and air. Therefore, there is an urgent need to contribute to the enhancement of the existing plastics waste management schemes. One of the solutions to this problem is the use of biodegradable polymers such as poly(lactic acid) (PLA) to produce twines for green houses. Since these twines are compostable, no separation procedure of the greenhouse waste is needed.

Nevertheless, PLA twines do not degrade as quickly as the organic compounds therefore their degradation needs to be accelerated by extending the period in the composting tunnel, though this is an expensive solution. As alternative, this project aims to accelerate the degradation process by the use of appropriate catalyst.

2.1.1 Conditions inside the greenhouse: Working conditions of the twines

Working conditions of the twines in the greenhouses include a high light transmission between 70 % and 81 %. In addition, some greenhouses also have the ability to control the relative humidity (between 50 % and 70 %) which is an important parameter due to the hydrolytic degradation of PLA [5].

PLA is UV resistant [4] which a required property of the material to be used in the greenhouse. In the summer time, the temperature inside some greenhouses might increase up to 40 ºC, so the degradation of the twines should not take place at this temperature.

The twines should resist to the air pollutants and the pesticides that might be present in the greenhouse environment [5].

2.1.2 Conditions of the compost and composting process

Compost is a biological, humid environment where the degradation of organic matter occurs. Due to its physical and nutritional structure, the microbial population in the compost is diverse. Controlled biological decomposition of the organic matter into inorganic one made by microorganisms under aerobic conditions, is called a composting process [6].

This process has several stages [6]: the first one is the mesophilic phase (20 ºC < T < 40 ºC) where microorganisms break the simple molecules resulting from the hydrolysis. Then between 40 ºC and 70 ºC, a thermophilic phase occurs with an increasing microbial activity (which generates heat). At the end of this phase, the temperature decreases to ambient. In this third mesophilic phase the degradation happens at a slower rate until the organic carbon is converted to carbon dioxide. Decomposition and humification take place at the same time to degrade organic matter.

PLA composting time is reported to be between 45 and 60 days under industrial conditions [7]. The degradation in soil is much slower as the composting environment has a higher moisture content and the temperature range is higher. These conditions promote the PLA hydrolysis and assimilation by thermophilic organisms [8] [9] [10].

2.1.3 Differences between poly (lactic acid) (PLA) and polypropylene (PP) twines

PP and PLA are primarily distinguished by the raw material type: the former one being produced from fossil-fuel derivatives and the latter PLA is produced from renewable feedstock. This is an advantage of PLA over PP as the life of the product as a whole is more is environmentally friendly [4].

The other downside of products resultant from fossil fuel is that they depend on oil prices. On the other hand, PLA price is currently set for a year as its feedstock is renewable [4].

PP is UV sensitive and PLA is UV resistant, which is an advantage considering the greenhouses environment [4].

The mechanical properties of PP and PLA twines differ slightly as the former has a higher tenacity and they are more chemical resistant whereas the latter has a lower tenacity. The hydrolysis test comparing PP with PLA composites at 80 ºC showed that the former did not show

any signs of degradation, whereas the latter composites loss a total of 80 % of the initial mass [4] [11].

Over the years, the price gap between conventional polymers and PLA has been shrinking due economies of scale. NatureWorks' Ingeo, the largest PLA manufacturer, claims that 140,000 tons·year^{-1} PLA production means 60 % less greenhouse gases and less 50 % of non-renewable energy when compared to PS or PET [12].

2.2 Poly(lactic acid) (PLA)

One of the most positive points of PLA production in comparison with the other hydrocarbon-based polymers is the decrease of CO_2 emission, because it is produced from natural sources such as crop residues (straw, husks, and leaves) or corn, sugar cane, potatoes due to the presence of starch in these plants.

Poly(lactic acid) is a biodegradable aliphatic polyester with a hydrolysable backbone due the presence of ester groups presence. The monomeric unit of PLA is represented in Figure 1 [13]. PLA was discovered in 1932 by Carothers (at DuPont). He was only able to produce a low molecular weight PLA by heating lactic acid under vacuum while removing the condensed water [14].

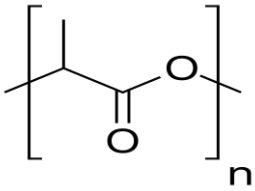

Figure 1: Monomer of poly(lactic acid)

PLA has mechanical properties similar to the petrochemical based plastics polystyrene (PS), polyethylene terephthalate (PET) and PP and it has favourable properties such as: simple production, biocompatibility, null toxicity, high mechanical strength and thermal plasticity. PLA polymer is also compostable under in industrial conditions. These characteristics turn PLA in a promising material to help to reduce the fossil energy consumption, reduce the municipal solid waste and help to close the carbon cycle [7] [8].

2.2.1 PLA resin production

Firstly, the PLA monomeric unit, the lactic acid (2-hydroxy propionic acid) subsists as two stereo isomers in nature: L-lactic acid and D-lactic acid (Figure 2) [8].

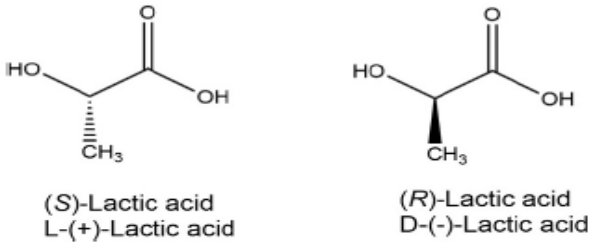

Figure 2: Lactic acid stereo isomers: L-lactic acid and D-lactic acid

Lactic acid can be produced by bacterial carbohydrates fermentation or by chemical synthesis. The latter process generates the lactic acid only in the meso-form which is optically inactive.

There are three pathways to produce high molecular weight PLA: direct polycondensation, azeotropic dehydrative condensation polymerization and ring-opening polymerization.

The direct polycondensation, which is considered the most cost effective process, has three main steps: free water removal, oligomer polycondensation and melt polycondensation of high molecular weight PLA.

Azeotropic dehydrative condensation polymerization or direct polycondensation in an azeotropic solution does not use chain extenders or adjuvants. While the polymer is produced by a direct condensation, the produced water is continuously removed by the azeotropic distillation. This method requires a catalyst, which is normally added with diphenyl ester. At the end, the polymer is isolated as obtained or it is dissolved to be precipitated for further purification.

The ring-opening polymerization method is a solvent free multi-step process. The lactic acid is condensed to low molecular weight pre-polymer, which is turned into lactide during controlled depolymerization. After this step, the lactide ring is opened and then the product is polymerized with the help of a metal complexes based catalyst.

Depending on the enantiomers composition and on the thermal history, the polymer can be amorphous (D-isomer amount > 6 %) or semicrystalline (D-isomer amount < 6 %) in its solid state. If the sample is only composed by the L-isomer, it is considered crystalline. The optical composition and therefore crystallinity affects important PLA properties such as melting temperature (T_m), glass transition temperature (T_g) and mechanical properties. Moreover, as the percentage of D-isomer increases these temperatures decrease. Depending on the application, high crystallinity might be desirable due to its improvement in heat and chemical resistance of PLA as well as its higher strength and permeability. It is clear that amorphous domains increase the degradation rate of PLA [8] [7].

These mechanisms are presented in Appendix Figure 1 [8] in Appendix 1.

2.2.2 Applications and worldwide producers

Initially, PLA was only used for medical applications (e.g. medical implants and surgical sutures) due to its high production cost. As lactic acid began to be produced by starch bacterial fermentation the production cost drastically dropped and as a result, its applicability increased.

Nowadays, PLA is used in the food-packaging for short-life products (as it is considered Generally Recognized as Safe by the United States Food and Drug Administration) including bottles, bags and food containers, in fibre production, in electronic field (i.e. flame retardant alloy used in laptops), as wrapping films and in tapes manufacture. It also has some applications in cosmetics and in 3-D printers [8] [7].

2.2.3 Production of PLA fibres

The overall production process has several stages: extrusion, draw and quenching, stretch, thermal stabilization and take-up of the fibre in a bobbin. The overall process will be explained with a special attention being given to the extrusion and stretch stages [15].

2.2.3.1 Extrusion

The process of PLA fibres starts with an extrusion step in a rotating screw. Usually, a general-purpose screw of L/D ratio (i.e. ratio of flight length of the screw to its outer diameter) between 24 and 30 is used. It is recommended to use polyesters or PS extruders to process the PLA resins as substantial torque is required for this process [15].

The resin is transported by the rotation of the screw. The extrusion happens as the material is both slipping on the screw and adhering completely to the inlet cylinder [15].

The extrusion process gives the heat to the melt of the PLA resins. Most of the heat is provided by the friction between the screw and the barrel, although some heat is given by heater bands wrapped around the latter. These heaters are usually set at temperature range between 40 and 50 ºC higher than T_m of PLA in order to ensure that all the crystalline domains are melted and the optimum viscosity is achieved [15].

The extrusion at high temperatures might thermally degrade the PLA, so the process parameters should be carefully controlled. Thermal degradation might lead to lactide and acetaldehyde as by products [8].

Apart from being heated and melted, the material is also compacted and compressed in order to allow it to flow through the ducts and filters placed before the die head.

A scheme of a single-screw extruder is presented in Appendix Figure 2 (Appendix 3) [8] [15].

2.2.3.2 Stretch process

The stretch process is a step which is going to give the fibre the appropriate tensile mechanical properties (tenacity, elasticity modulus, elongation) for the desired application. The stretch is a continuously applied elongation deformation quantitatively represented by the stretch ratio, R_s calculated from equation 1 [15].

The process is outlined in Appendix Figure 3 (Appendix 3). The L roll is rotating, picking up and dragging the filaments at is peripheral speed (V_L). A tensioning device, T, is preventing the filament from slipping onto the roll L surface. H is also a rotating roll. It rotates and stretches the filament at V_s stretch rate. C is a thermoregulated filament heating system [15].

If $V_S > V_L$:

$$R_s = {}^{V_S}\!/_{V_L} = {}^{T_f}\!/_{T_S} \quad \textbf{(1)}$$

where T_f and T_S are the values of the filaments titres when entering and exiting stretch stage.

The fibre degree of orientation and crystallinity is related to the stretch ratio. The stretched fibres tend towards a single orientation degree which is independent of the maximum stretch ratio value (how much the fibre can be stretched) [15].

2.2.3.3 Monofilaments overall process

The Appendix Figure 4 (Appendix 3) presents the outline of the following stages after the extrusion: 1. Spinning, 2. Quenching and solidification, 3. Draw, 4. Heating, 5. Stretch, 6. Thermal stabilization, 7. Recovery, 8. Winding [15].

Normally the spin rate (V_f) is low, which assures that as the monofilament comes out as a straight fibre after the spinning stage. Otherwise, the fibre tends to curl due to the spinning stress. Then, the monofilament is cooled and solidified in cool water and subsequently it is dried by jets of air. Afterwards, a thermoregulated oven brings the monofilaments to the stretch temperature. Subsequently, a second oven and a third powered roll system, with lower

peripheral speed than the stretch rolls, will guarantee the thermal stabilization. The process ends with the cooled monofilaments being separately wound on the bobbins [15].

2.2.4 Degradation pathways

The PLA degradation is known as a two-step mechanism. The first one is the abiotic process (hydrolysis) and the second one is the biotic step (i.e. microorganisms decompose the hydrolysis end products). The later one might be under aerobic or anaerobic conditions. This two-step mechanism is unique for biodegradable polymers [7].

2.2.4.1 Composting process

2.2.4.1.1 Hydrolysis

In the presence of water or aqueous solutions, the main chain ester groups of PLA are cleaved [16]. This random non-enzymatic chain scission followed by a chain-end hydrolysis (represented by Equation 2) causes a decrease in the molecular weight due to the release of oligomers and monomers.

$$-COO + H_2O \rightarrow -COOH + OH- \quad \textbf{(2)}$$

This is a self-catalysed reaction since the carboxylic acid end group with pKa around 3 acts as acid catalyst in hydrolytic degradation. Amorphous PLA chains are the starting point of the hydrolysis as the water molecules diffusion rate is higher in these regions than in the crystalline ones. With a decrease in molecular weight the tensile strength of the material drops [7] [8].

Several factors influence the hydrolysis rate, the most important ones are: temperature, pH and relative humidity (*RH*). The hydrolysis degradation rate increases with temperature as the chain scission is accelerated. The medium pH also influences the hydrolysis rate: both hydronium and hydroxide ions catalyse the reaction. It is also reported that with a high *RH* (>60 %) the rate increases due to faster absorption of water molecules [7] [8] [16].

The hydrolysis mechanism is presented in Figure 3 [8].

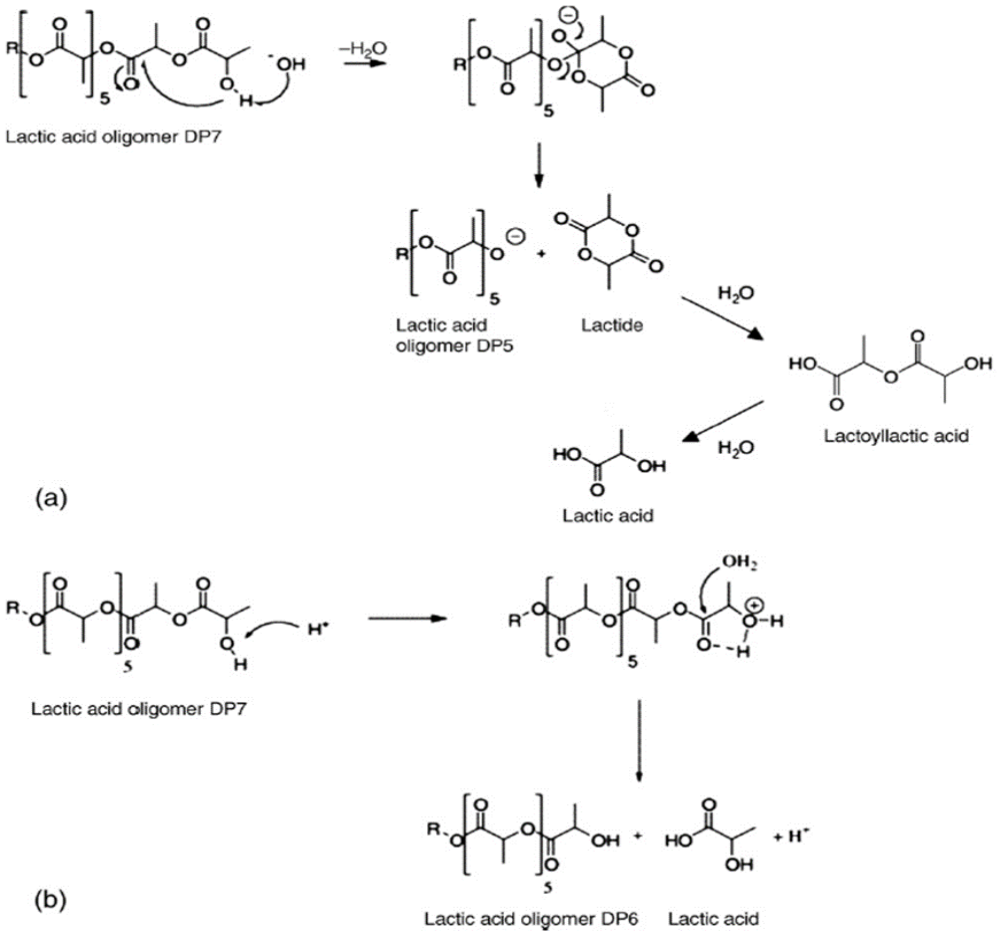

Figure 3: Hydrolytic chain cleavage mechanisms of PLA in alkaline (a) and acidic media (b)

2.2.4.1.2 Microorganism digestion

After the PLA fibre is degraded into low M_W compounds (≤ 10, 000 Da), microorganisms are ready to proceed with the biotic degradation. Different types of microorganisms are capable to degrade these low molecular weight compounds as presented in **Erro! A origem da referência não foi encontrada.** [8] [7] [17] [18].

2.2.4.2 Thermal degradation

PLA thermal degradation takes place above 200 ºC in a nitrogen atmosphere as intra- and intermolecular ester exchange, *cis*-elimination, radical and concerted non-radical reactions occur as well as random scission, unzipping polymerization and intermolecular transesterification. Low molecular weight products appear as result of these reactions [8].

This degradation is influenced by several factors such as initial M_W, moisture amount and residual polymerizing catalysts. The moisture amount, the temperature and residence time in the extruder during the entire process might decrease M_W and consequently stress and strain at break due point [8].

The presence of residual metals affects PLA onset degradation temperature. The reported onset temperature order is Fe > Al > A > Sn [8]. It is known that A catalyses intermolecular transesterification that produces linear oligomers and selective unzipping depolymerization of the cyclic oligomers that will result in lactides [19]. A higher thermal stability is achieved with the onset temperature increase due to a reduction of active sites on the chain end [8] [20].

These mechanisms are presented in Figure 4 [8].

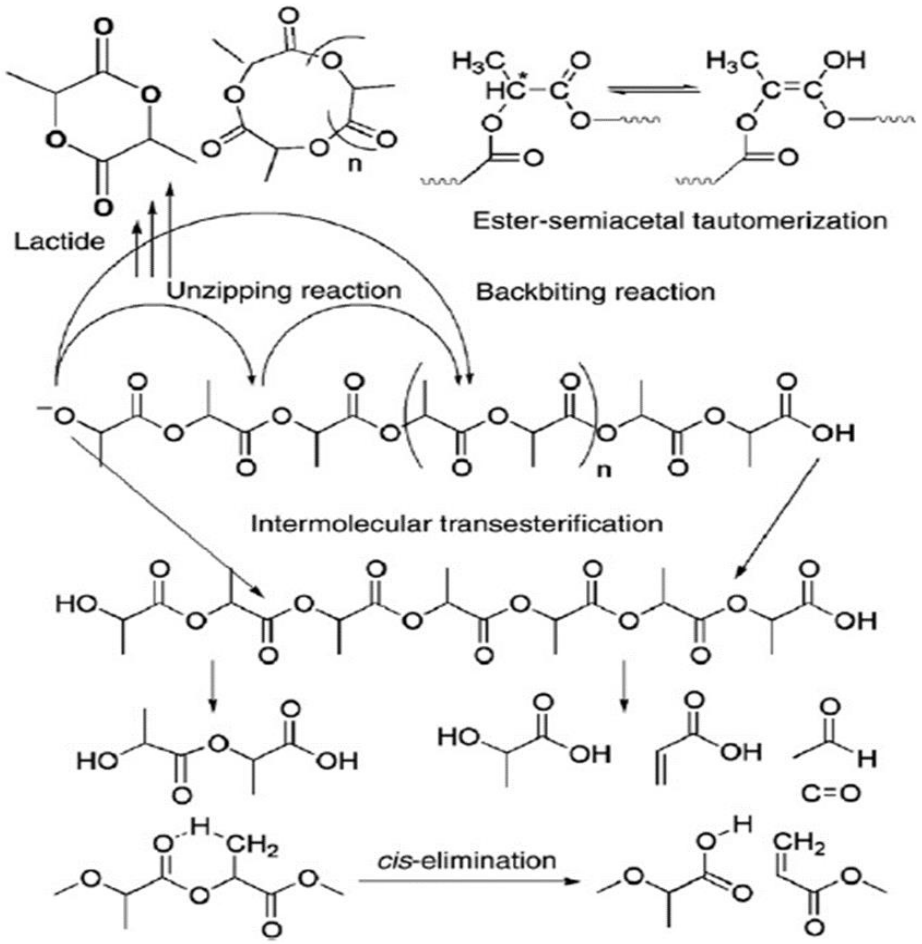

Figure 4: Thermodegradation PLA mechanisms

2.3 Catalysts for hydrolytic degradation of PLA twines

The catalyst is defined by the International Union of Pure and Applied Chemistry as "a substance that increases the rate of a reaction without modifying the overall standard Gibbs energy change in the reaction" [21]. The catalysis process happens when the reaction rate increases (due to a promotion of alternative reactional mechanism) with the catalyst regeneration after each catalytic step. The catalyst does not influence the thermodynamical equilibrium of the overall reaction but it can affect its yield and selectivity [22] [23].

There are several catalysts types, with different active sites and surface chemistry [24]. Four different types were studied in the present work: oxides, zeolites, clays and carbon based

catalysts). The functionalisation of A and F with the acidic sites was also considered in order to improve the activity of the catalysts in hydrolytic degradation of PLA fibres.

The hydrolytic degradation process is a heterogeneous catalytic process as one of the reactants is water and the catalyst is in the solid state [22].

2.3.1 The role of the catalysts in the PLA twines and the material requirements

In the present work, the catalyst will be introduced in the PLA twines during extrusion process. The goal was to increase the rate of the hydrolytic degradation of these twines and to minimize the residence time of the waste from the greenhouses containing a mix of PLA twines and green matter in the composting tunnel.

The sought catalytic material in the present application should not show any activity up to 40 ºC, which is the maximum temperature that might be reached inside the greenhouse, as it was mentioned before. It should be noted that the atmosphere in the greenhouse contains a lot of moisture [5], which together with an active catalyst could trigger the hydrolysis of the PLA twines. On the other hand, the catalyst in the twine should show a high activity at 70 ºC, which is the composting thermophilic stage temperature, as it was denoted in Section 2.1.2. Furthermore, the catalyst should also be UV resistant, similarly to the pure PLA twines and preferably it should be food contact approved as the twines are in contact with the vegetables, as it was mentioned in Chapter 1.

Heterogeneous catalysis usually occurs at solid surface active sites. The catalyst should have upright accessibility to the reactant (the fibre in this case) [22] [24]. To fulfil this last condition, that the catalyst would be homogenously distributed in the interior of the fibre and on the surface of the fibre to ensure the good accessibility.

Hydrolysis depends on water diffusion rate in the structure of PLA fibre. The chosen catalysts should ensure that the diffusion rate does not decrease. The rate can decrease if the catalyst forms branched polymer structures with hydroxyl terminal groups. These groups will probably form hydrogen bonds which will occupy the free space where the water would diffuse [25] [26]. The catalysts on their own can also occupy space in the polymer structure which would decrease the water diffusion [27].

Zeolites, A, E and clays were already studied as suitable catalysts for PLA. Zeolites and clays are known as adsorbents and to provide increase of mechanical properties to PLA nanocomposites [8] [30]. A accelerates the degradation of PLA nanocomposites [28]. E is reported to have a “reinforcing effect” in PLA films [29]. However, they were used in nanocomposites and films not in fibres.

3 Materials and Methods

3.1 Materials

3.1.1 Catalysts

Three main groups of commercial materials were selected to be tested; oxides (A, E, G) clays (C, I, J, K), carbons (D, F, F-20, L), zeolites (B, H) and polymers, due to their diverse properties for application as catalysts in the hydrolysis of PLA twines, due to their surface. Two different polymers were studied in this project: Polymer_A and Polymer_B which were selected mainly due to their higher rate of degradation under compost conditions.

A and F were functionalized applying treatments with acids (citric acid and nitric acid, respectively). The procedures will be described later in Section 3.3. In total, 14 different catalysts were screened in hydrolytic degradation of PLA twines during this project.

The amount of catalysts (in the powder form) incorporated in the PLA fibre was 1 wt %. The amount of polymers, which were incorporated in the fibre was 3 wt %, because it is known that this amount should not introduce significant changes in the mechanical properties of the PLA fibre, but potentially could accelerate the degradation process. Below 3 wt % changes are not seen and above 3 wt % PLA fibre morphology changes. Two different polymers were studied in this project: Polymer_A and Polymer_B as described below.

Polymer_A can be extracted from bacteria cell and has higher biodegradability in composting plants in both aerobic and anaerobic environments. It is also ultra-violet resistant which is very relevant mainly in the studied application as twines for growing tomatoes in the greenhouses. Moreover, Polymer_A is compostable over a varied range of temperatures [31].

Polymer_B is certified biodegradable polymer in industrial conditions according to DIN EN 13432 [32] which it can be used in agricultural ends. However, its efficiency in biodegradability depends on the surrounding environment and on its composition [33].

In order to prepare the samples, the polymers were introduced in the extruder hopper in the form of pellets following the procedure used for pristine PLA.

Process_Aid was used as a bonding agent between the catalysts (i.e. powder) and the PLA (i.e. pellets) in order to adhere the powder catalysts to the pellets and improving the homogenization process. 0.25 wt % of Process_Aid bonding agent was added to each of the fibre samples. In addition, PLA fibre with the same concentration of Process_Aid was produced and tested in order to study the possible influence of this agent on the degradation behaviour of the fibre.

3.2 Catalysts Functionalization with acids

3.2.1 A: treatment with Citric Acid

A was functionalized with citric acid following the modified method described in [34] in order to improve the catalyst performance, by introducing acidic active sites on its surface. Acidic sites are known to be active in hydrolysis of various biopolymers, e.g. cellulose [35] .

In short, 10 g of A were dispersed in 1 L of DI water and stirred continuously with a speed of 750 rpm for 15 min. In the meantime, a solution of 1 g of citric acid was prepared and ultra-sonicated for 15 min. Subsequently, the solution of citric acid was added to that of A. The final mixture was sonicated for another 30 min. Finally, the catalyst was washed by centrifuging for 30 min at the speed of 2200 rpm [34]. The functionalized A was left to dry overnight in a 100 ºC in a hot air oven. In order to assure that there was no unreacted citric acid present with the functionalized A was placed in a furnace at 300 ºC under 100 $mL \cdot min^{-1}$ nitrogen flow with a heating ramp of 5 $ºC \cdot min^{-1}$ and a soaking time of 1 h.

3.2.2 F: treatment with Nitric Acid

F was oxidized (carboxylated in a strong acid) in a liquid phase with 2 M HNO_3 (34.3 mL) for 5 g of F following the standard procedure described in [36]. This method is known to introduce a large number of carboxylic acid groups on the surface of carbon [36]. The oxidation was performed for 2 hours and the material was then washed with DI water using a Soxhelt with an extraction thimble (with 22 x 80 mm size) until the pH of the water after washing was similar to the pH of fresh DI water [37]. Finally, the sample was dried in a hot air oven overnight at 100 ºC.

3.3 Catalysts Characterization

3.3.1 Particle size distribution

The particle size distribution was measured because it was a very important parameter for sample preparation via extrusion. Essentially, the filter of the extruder is only appropriate for particles smaller than 20 μm. This measurement was done in a Beckman Coulter LS™ 200. This equipment works based on the light scattering theories and has a wide dynamic size range. The light scattering was optimized by the reverse Fourier lens optics of the equipment. The

Polarization Intensity Differential Scattering (PIDS) method was applied due to the submicron size expected for the particles [38].

Firstly, the suspensions of the powders were prepared using ethanol and sonicated for 15 min. It is very important for the powders to be well dispersed in solvents in prior to these measurements, because otherwise aggregates not the true particles are measured.

As C did not make a good dispersion with ethanol, other solvents were tried and finally, 2-propanol was used in the measurements for this catalyst.

3.3.2 Ball-milling

In case of two first samples (B and C), their particle sizes were larger than 20 μm, thus it was decreased by ball-milling. The frequency and the time were optimized from 15 s^{-1} and 15 min to the optimal values of the frequency of 20 s^{-1} during 25 min

3.3.3 Textural Characterization – N_2 adsorption at -196 ºC

The textural characterization of the samples was performed using a Quantachrome Autosorb IQ apparatus by N_2 adsorption/desorption measurements at -196 ºC. All the samples were outgassed at 150 ºC for 3 hours in vacuum, before the measurements. The cells were placed in a cryogenic N_2 bath while the analysis took place.

The Brunanuer-Emmett-Teller (BET) method was employed for the determination of surface areas (S_{BET}) of catalysts. Micropore volumes (V_{micro}) and external surface areas (of meso- and macropores; S_{Meso}) were found using the t-plot method, whereas the total pore volume (V_{Pores}) was obtained from the amount of N_2 adsorbed at a relative pressure (P/P_0) close to unity.

For the F and F-Func, pore size distribution was analysed by the Density Functional Theory (DFT) method. The F-20 pore size distribution was given by the catalyst supplier.

3.3.4 Thermogravimetric analysis Differential Scanning Calorimetry (TGA and DSC)

The thermogravimetric analysis measures the weight loss percentage in a range of temperatures to study the sample thermal behaviour. The differential scanning calorimetry intends to measures the melting temperature (T_m), melting enthalpy and glass transition temperature (T_g).

Thermogravimetry analysis was performed to quantify the amount of volatiles present in the treated catalysts and compare these results with the non-treated ones. Both F and F-Func and both A samples were heated in N_2 from 323 K until 1273 K at 25K min^{-1}. The samples

were heated until 1273 K in order to measure the amount of volatiles, which can be directly related to the amount of oxygen functional groups [34] [37] .

3.3.5 pH Point Zero Charge (pH_{pzc})

pH Point Zero Charge is a measure of the total acidity or basicity of the catalyst surface and it is also the pH value which has a null superficial charge.

This pH_{pzc} analysis was carried out for A. 0.01 M NaCl solutions with a pH range between 3 and 10 were prepared. The pH of these solutions was adjusted with HCl and NaOH (0.01 M). Two series of solutions were prepared in this experiment. One that involved 10 mg of A and 20 mL of the solutions with desired pH (5 flasks) and the other series called "blank", containing only the solutions (5 flasks).

After being agitated for 45 h at room temperature pH of flasks containing A material and those of corresponding blanks were measured. The pH_{pzc} was assessed from the point at which the curve pH_{final} vs $pH_{initial}$ intersects the line $pH_{final} = pH_{initial}$.

3.3.6 Fourier-Transform Infrared Spectroscopy (FT-IR)

Fourier-Transform Infrared Spectra for F and A samples were recorded using a Jasco 6800 spectrophotometer between 4000 and 400 cm^{-1} with a 4 cm^{-1} resolution in order to study the functional groups present on the surface before and after functionalization [34] [37]. The citric acid spectrum also recorded to for comparison and to confirm that there was not unreacted citric acid present in the A Acid Treated sample.

3.3.7 Scanning Electron Microscopy with Energy Dispersive Spectroscopy (SEM/EDS)

The scanning electron microscopy (SEM) uses a focused beam of high-energy electrons, which generate a variety of signals at the surface of solid samples due to the electron-sample interactions. These interactions give information about morphology and chemical composition [39]. The latter is determined by energy dispersive spectroscopy (EDS). This technique consists in a separation of the characteristic x-rays of each element into an energy spectrum which shows the abundance of a specific elements [40].

In order to characterize the morphology and the composition of the powder catalysts as well as the fibres with the addition of the catalyst a scanning electron microscopy with energy dispersive spectroscopy was performed using a High resolution (Schottky) Environmental Scanning Electron Microscope with X-Ray Microanalysis and Electron Backscattered Diffraction

analysis: Quanta 400 FEG ESEM / EDAX Genesis X4M (15 keV). The analysis was made in Centro de Materiais da Universidade do Porto (CEMUP).

Prior to the analyses, all the samples were coated with an Au/Pd thin film, by sputtering, using the SPI Module Sputter Coater.

The images were taken at different magnifications and two different detection modes were used to analyse the samples: secondary and back-scattered electrons [34].

3.3.8 Temperature Programmed Desorption (TPD)

Temperature Programmed Desorption analysis was performed for F and A non-treated and treated samples to evaluate the nature of the surfaces functional groups and to access the amount of oxygen introduced during functionalization [37] [34].

In short 150 mg of each sample was placed in a U-shaped quartz reactor and heated up until 1100 ºC in 25 $cm^3 \cdot min^{-1}$ of helium with a heating rate of 5 $ºC \cdot min^{-1}$. The analysis was performed using AMI-200 (Altamira Instruments). CO and CO_2 (molecular masses of 28 and 44 respectively) were monitored by a mass spectrometer (Dymaxion 200 amu, Ametek) [37]. The analyses were performed accordingly with the previously developed method at LCM [41].

3.3.9 Elemental Analysis (EA)

In order to analyse quantitatively the composition of the F samples, an elemental analysis was performed in a vario MICRO cube Elementar Analyser (amounts of hydrogen, carbon and nitrogen described as the percentage in a bulk of the material). The amount of oxygen in the samples was measured separately using a Rapid OXY cube Elementar Analyser [36].

3.4 Hydrolysis Tests

3.4.1 Experimental Set-Up

The hydrolysis tests were carried out using a water bath shaker. The bath has 10 different positions for the test bottles. To make sure that all of the places had the same reaction conditions, a hydrolysis test with a benchmark PLA fibre was performed. This test was also done to evaluate the time needed for the first signs of the fibre degradation. The control test was performed at 70 ºC, (which is a standard composting conditions temperature), knowing that the temperature increase improves the fibre degradation.

Five glass bottles were filled with 150 mL of ultrapure water and with 10 pieces of 25 cm each of pristine PLA fibre. A test bottle with ultrapure water and no fibre was also placed in the water bath shaker to control the CO_2 from the overhead of the test bottles. The bottle caps were not fully closed in order to simulate as closely as possible, the composting conditions. For the following hydrolysis, 6 and 7 bottles with fibres were used at the same time. The 7 bottles scheme is presented in the Figure 5.

The control test showed that the results slightly differed within positions so in the following tests the fibre flasks were rotated clockwise every time a sample was taken to even the conditions. The reference water flask stayed in the same spot during all the experiments.

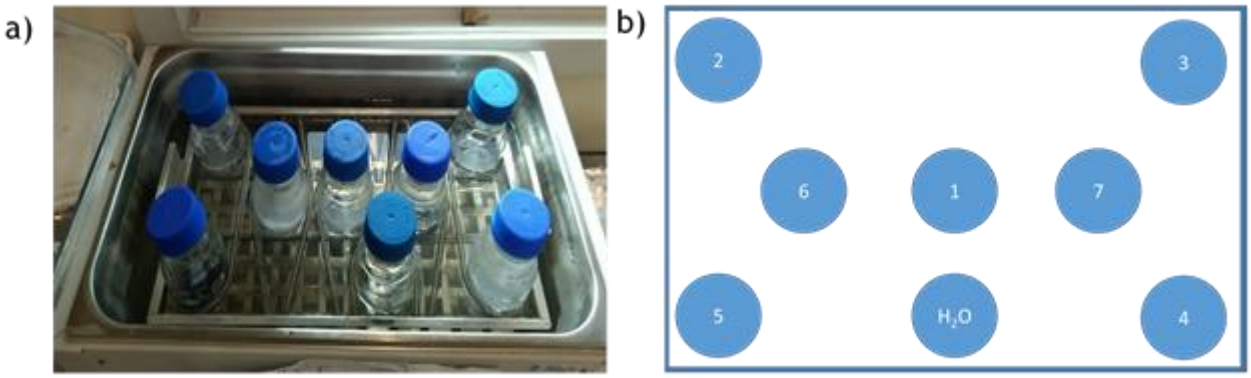

Figure 5: a) 7 bottles with fibres b) Positions numbers

3.4.2 Total Organic Carbon (TOC)

Total organic carbon content (TOC) is the total amount of carbon from covalently bound sources [42].

The dissolved total organic carbon concentration was measured in a TOC-L CPH SHIMADZU. Besides pH, TOC was used to measure the reaction extent due to the expected increasing presence of COOH groups with advancement of reaction.

3.4.3 Thermogravimetric Analysis and Differential Scanning Calorimetry (TG and DSC)

The thermogravimetric analysis was carried out in a NETZSCH STA 409 PC/PG equipment.

During the control hydrolysis with the pristine PLA fibre, three methods were carried out to find the best results and in a shortest possible time.

First, the samples were heated in N_2 from 323 K to 873 K at 25.0 $K \cdot min^{-1}$. After analysis of the DSC data, it was not possible to observe any changes in the peaks so it was decided to

modify the heating program until measurable changes could be clearly seen. The optimized heating programme was: starting to heat in N_2 at 299 K at 5.0 K·min^{-1} to 473 K and from 473 K to 873 K at 25.0 K·min^{-1}. From 873 K to 1073 K the samples were heated in air in order to burn the remaining material.

3.4.4 Gel Permeation Chromatography (GPC)

Gel Permeation Chromatography is a type of category of high performance liquid chromatography used to determine the molecular weight distributions of polymers and relate these parameters with different polymer properties. This method separates molecules based on size which is why GPC is also known as size exclusion chromatography [43].

Number average molecular weight, M_n, and weight average molecular weight, M_W, were calculated and analysed as the most relevant data to compare between the samples. M_n influences the thermodynamic properties and M_W is directly related with the polymer toughness [43].

Each sample was prepared with approximately 10 mg of fibre and 1 mL of tetrahydrofuran as a solvent. The samples were then ultra-sonicated until the fibre was dissolved. The dissolved sample was filtered through a hydrophobic PTFE 0.1 μm filter membrane to a new flask that was placed in the GPC Waters Alliance e2695. The injection flow was 1.0 mL·min^{-1} and the system pressure was 650 psi.

3.5 Tensile Tests

Tenacity (breaking force of the fibre divided by its titre; gf·den^{-1}) and elongation (length variation when stress is applied; %) are important fibres' mechanical properties [44]. To analyse how these properties, vary with the presence of the catalysts, temperature changes or hydrolysis, tensile tests were performed in a Zwick Roell Z005 dynamometer.

The trials had a 500 mm·min^{-1} speed and the gauge length was 500 mm getting a relative speed of 1-gauge length·min^{1} (100 %·min^{-1}).

The rupture force, runnage of the fibre and the moving head dislocation were the data used by the equipment software to calculate tenacity (g·den^{-1}) and elongation (%).

To check for changes suggesting an early thermal decomposition, the fibres were left in the lab oven for 12 h at 55 ºC. Then, tensile tests were performed to verify any changes of mechanical properties.

4 Results and Discussion

4.1 Catalysts Characterization

4.1.1 Particle size distribution

These distributions were all measured in water. The comparison of particle size distribution is shown in Figure 6. The most relevant catalyst particle distribution is presented in separate graphs in Appendix 4.

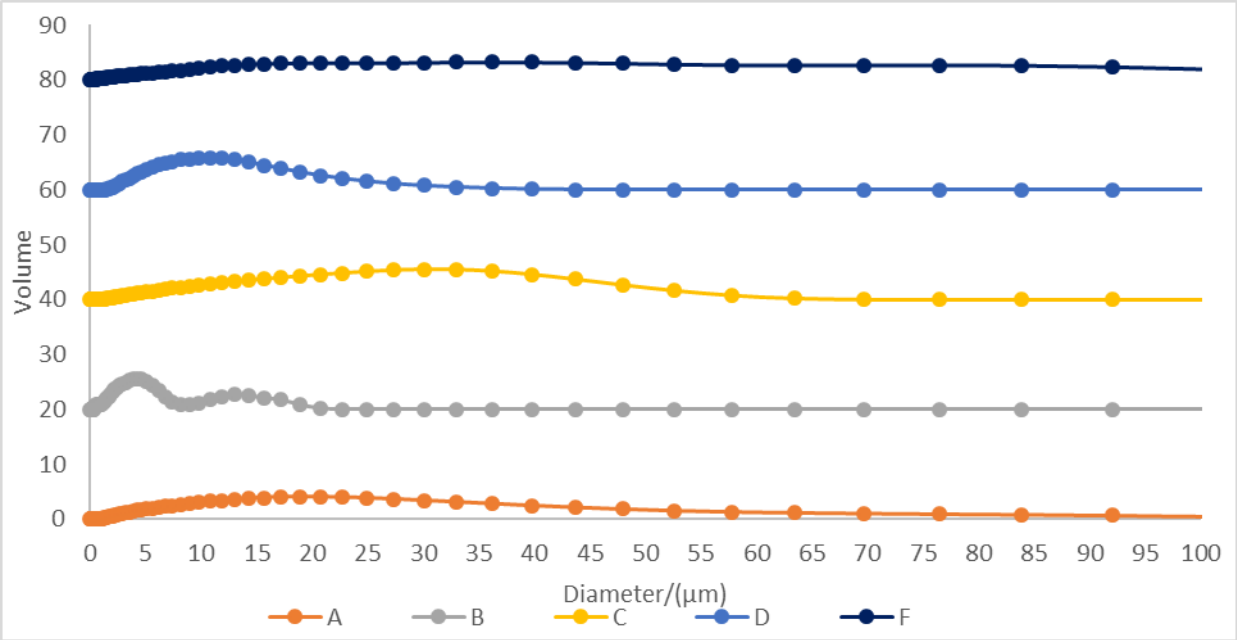

Figure 6: Particle size distribution comparison of 5 representative catalysts

As it was mentioned in Section 3.3.1., the extrusion filter was only suitable for particles with diameters under 20 µm. Considering this parameter, 6 catalysts were selected for further study: A, B, C, J, D, F.

As mentioned in Section 3.3.1., these 5 samples particle size distributions were remeasured in an ethanol suspension (propanol was used for C) and then the ball-milling program was applied to B, C and J. After ball milling, J particle size was still too broad so this catalyst was excluded from the study and the C clay was found to fulfil the particle size requirements.

Section 3.2. explains the catalysts functionalization applied here which resulted in two new samples (F-Func and A Acid Treated).

The 5 representative catalyst particle size distribution is shown in Figure 7.

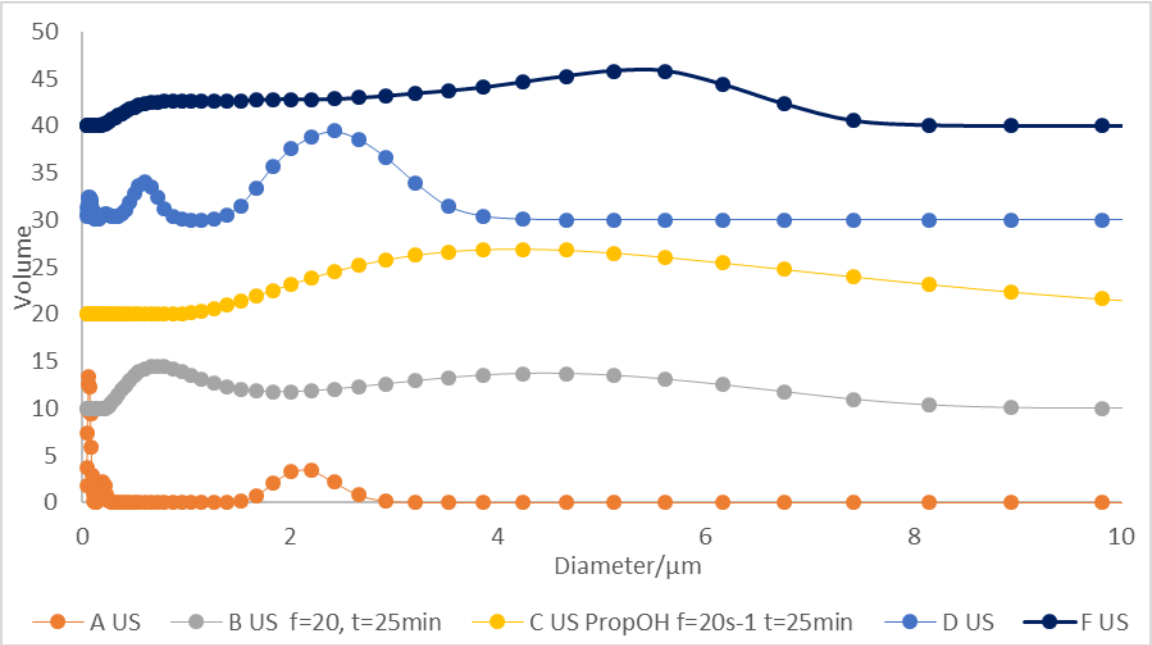

Figure 7: 5 representative catalysts final particle size distribution

4.1.2 Textural Characterization – N_2 adsorption at -196 ºC

N_2 adsorption and desorption at liquid nitrogen temperature were performed to measure the specific surface area and the pore size of the samples. The A and the F isotherms are presented in Figure 8. The remaining isotherms are gathered in Appendix 5.

From the A isotherm analysis, it is possible to verify the lower amount of micropores. The existent porosity in the A sample consists mainly of mesopores. The F isotherm differs from the first one presented as F presents micropores.

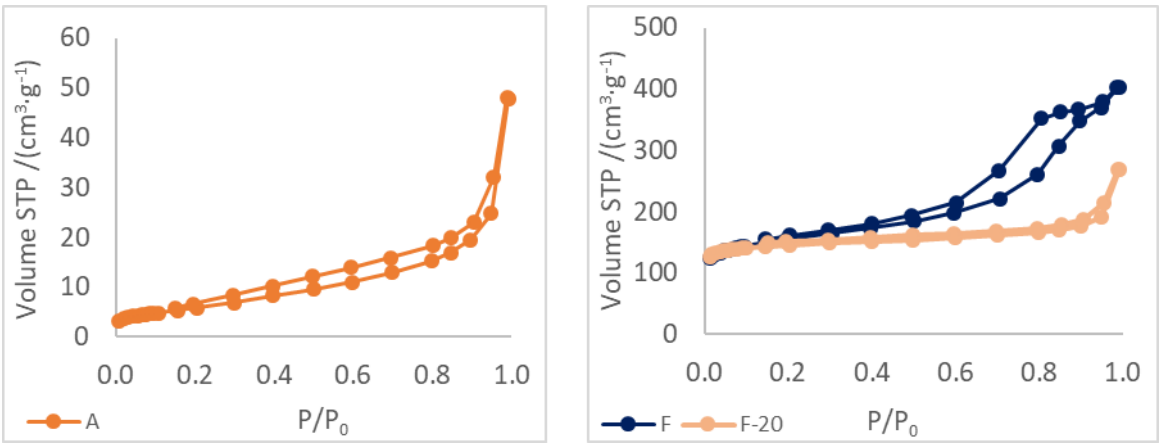

Figure 8: Adsorption isotherms of A, F and F-20 catalysts

From the software data it was possible to determine the surface area (S_{BET}) applying the B.E.T. method. With the t method it was possible to obtain the mesopore area (S_{Meso}) and

the micropore volume (V_{micro}). The total pore volume (V_{pores}) was also given by the software. The data is presented in Table 1 and confirms the preliminary isotherms analysis.

Table 1: Catalysts textural characterization by the B.E.T. and t plot methods (P/P_0 = 0.99 atm)

Sample	f (s^{-1})	t (min)	S_{BET} (±10) ($m^2 \cdot g^{-1}$)	S_{Meso} (±5) ($m^2 \cdot g^{-1}$)	V_{micro} ($cm^3 \cdot g^{-1}$)	V_{pores} ($\times 10^{-1}$) ($cm^3 \cdot g^{-1}$)
A	-	-	22	21.7	0.0	0.7
A Acid Treated	-	-	22	21.7	0.0	2.8
B	20	25	685	54.2	0.3	4.3
C	20	25	7	6.8	0.0	0.4
D	-	-	481	430.6	0.0	3.1
F	-	-	532	221.1	0.1	6.2
F-Func	-	-	535	232.2	0.2	6.0
F-20	-	-	446	87.9	0.2	4.2
G	-	-	8	7.8	0.0	0.2

However, the surface area in both samples remained the same after functionalisation treatment it was expected, that both non treated samples (A and F) would have higher surface area than the respective treated samples (A Acid Treated and F-Func).It was reported for carbon catalysts that liquid phase (especially carried out indirectly using Soxhlet) did not induce change in textural characteristics [36]. In fact, the lack of changes in specific surface area shows that the functionalization was done properly modifying inly the surface chemistry of the samples.

Although it was possible to get values from the software of the E isotherm analysis, it is possible to observe that measurement was not correctly done, probably because the surface area is too small (S_{BET} < 5 $m^2 \cdot g^{-1}$) [29] for the equipment measurement capacity.

In Figure 9, it is possible to verify that the pore distribution in F samples did not change after the functionalization. It might had occurred that the new groups are mostly in

surface and did not occupy the pores, which will be verified with other characterization techniques.

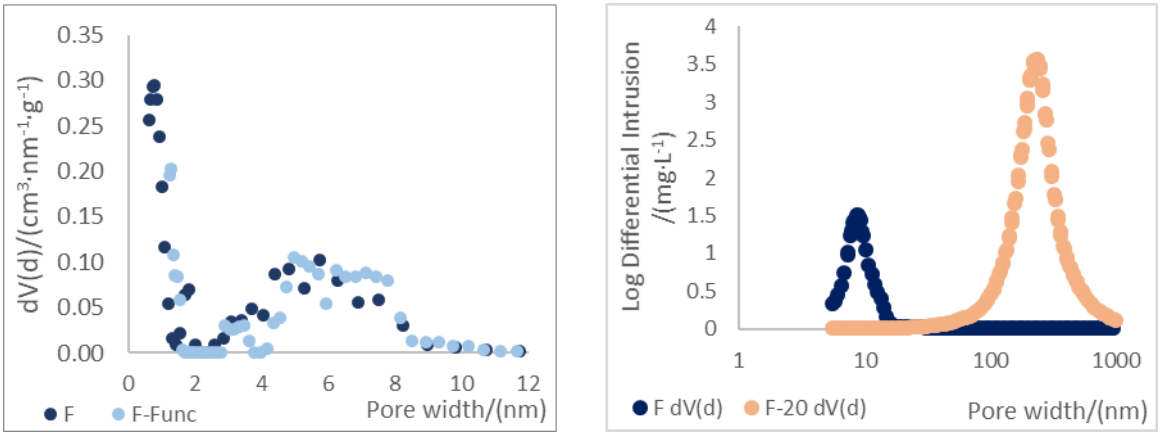

Figure 9: Pore size distribution: F comparison by the DFT method and different size pore distribution performed by Dr[a] Ana Arenillas de la Puente by mercury porosimetry

It is possible to verify the pore size influence of the carbon Fs samples. The isotherms forms (Figure 8) are different as the F-20 S_{BET} is 16 % lower than the F S_{BET} and the F-20 S_{Meso} is 60 % lower than F S_{Meso}.

4.1.3 Thermogravimetric Analysis (TGA)

Thermogravimetric analysis was performed with to all the catalysts to verify the percentage of weight loss (Total Weight Loss, %), maximum peak temperature (T_{peak}) and depending on the catalysts the amount of present volatiles or the amount of ashes (B and C).

Table 2: Results from thermogravimetric analyses of the selected catalysts

	A	A Acid Treated	Citric Acid	B	C	D	E	F	G	F-Func	F-20
T_{onset} (°C)	317	354	229	109	290	153	165	82	236	236	51
T_{peak} (°C)	221	448	242	158	350	61	50	123	541	241	123
Total Weight Loss (%)	0.1	0.4	96	16	37	1.5	-2.5	8.2	-2.3	71	6.6

Table 2 presents an overview of the results and the rest of the results can be found in Appendix 6.

Thermogravimetric analysis of treated and non-treated samples is presented in Figure 10. It is possible observe an increase of weight loss in the treated F. The difference between F and F-Func, which can be attributed to the presence of oxygen functionalities on the surface of F-Func sample. Comparing both non treated F samples, it is possible to observe that the pore size influences the weight loss as F lost 19.5 % more mass than F-20.

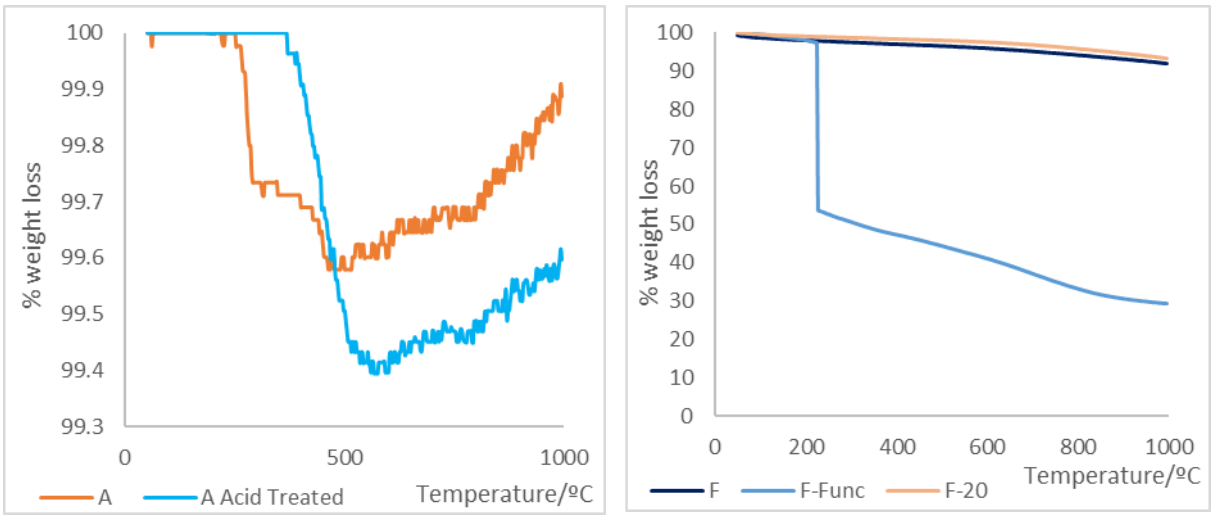

Figure 10: Weight loss percentage comparison between the non treated and the treated

In both Appendix Figure 17 and Appendix Figure 18, it is possible to observe that B and C weight loss is higher than the other non-treated catalysts. Zeolites and clays are used as adsorbents so most of their weight loss is due to water and gases adsorbed from the surrounding environment [45] [46]. D (Appendix Figure 19) has a similar behaviour to the non treated F because both of these materials are carbon catalysts [47]. From Table 2 it is possible to observe that both E and G present weight increase as probably they would need more time on standby temperature. However, it was not expected that these oxides would lose more than 1 % as they are thermally stable due to theirs crystalline structures [48] [49].

4.1.4 pH Point Zero Charge (pH_{pzc})

As mentioned in Section 3.3.5, the basicity or acidity of the A surface was measured. The observed pH_{pzc} value was 7.2. It was according with the expected as its surface was reported to be slightly basic due to presence of –OH surface groups [34].

4.1.5 Fourier-Transform Infrared Spectroscopy (FT-IR)

The A Acid Treated sample was expected to have carboxylic acid groups, ester linkages and hydroxyl groups. The F-Func should have hydroxyl groups, carboxylic anhydrides and carboxylic acid groups.

In Figure 11, it is possible to observe both A samples spectra and the citric acid (CA) spectra. The pristine A shows mainly –OH stretching vibrations (450 cm^{-1} and 3450 cm^{-1}). The A-O bond might be observed close to 400 cm^{-1}. The CA spectra shows the typical broad bands between 600 and 1800 cm^{-1}. The C=O stretching bond appears around 1650 cm^{-1} and the peaks assigned to C-O stretching appear between 1100-1200 cm^{-1}. The CH_2 stretching vibrations appeared at 2865 cm^{-1} and the non dissociated O-H groups appeared at 3500 cm^{-1}. The A Acid Treated showed that the interaction between CA and A let to the C=O stretching peak shift to 1200 cm^{-1} as a result of the formation of intermolecular hydrogen bonds between –OH and C=O of CA with A surface. New peak appeared over 2800 cm^{-1} corresponding to the –OH groups [34].

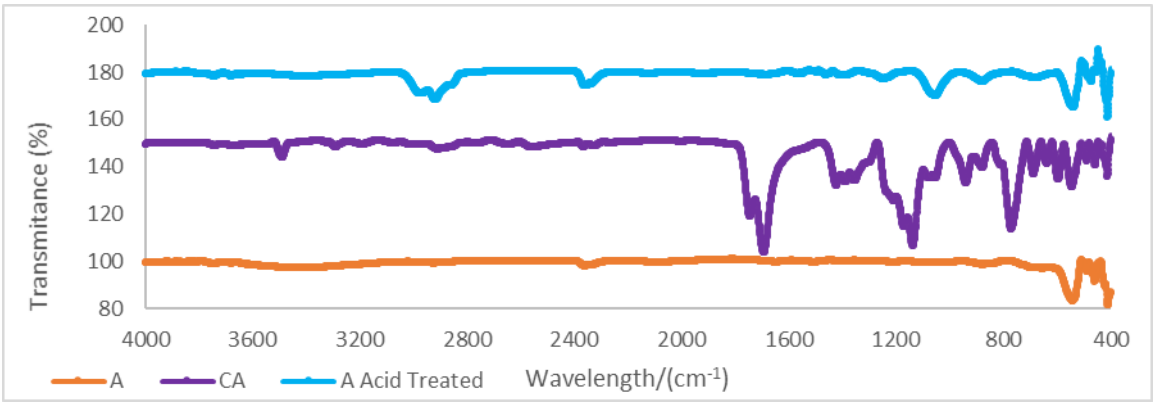

Figure 11: A samples FT-IR spectra

Figure 12 shows both F spectra. The biggest difference in these samples is the peak intensity confirming the oxygen surface groups insertion after the functionalization. From 600 cm^{-1} to 1200 cm^{-1} it is possible to observe a broad peak which might include C-OH and –OH from phenolic structures, C=O from carboxylic acids and anhydrides. Between 1620 and 1680 cm^{-1} it is possible to observe the C=C from the aromatic structure, carboxylic acids and lactones [36].

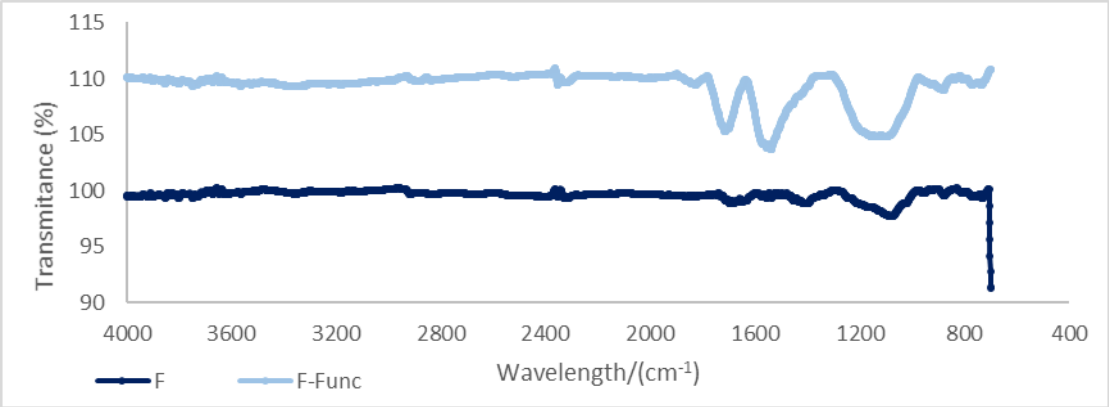

Figure 12: F FT-IR spectra

4.1.6 Scanning Electron Microscopy with Energy Dispersive Spectroscopy (SEM/EDS)

A SEM analysis was performed to characterise the catalyst structure and to obtain additional information about the particle sizes. In Figure 13 the particle size measured in the chosen area of the sample was much smaller that the particle size distribution indicated in Figure 7, measured by Polarization Intensity Differential Scattering

Figure 13 presents a) A and b) E as they are two materials reported to have different effects in PLA fibre, respectively – A promotes degradation [28] and E is known as a "reinforcing particle" for PLA fibre [29]. Micrographs of these catalysts shown in Section 4.3.4. to confirmed the reported effects.

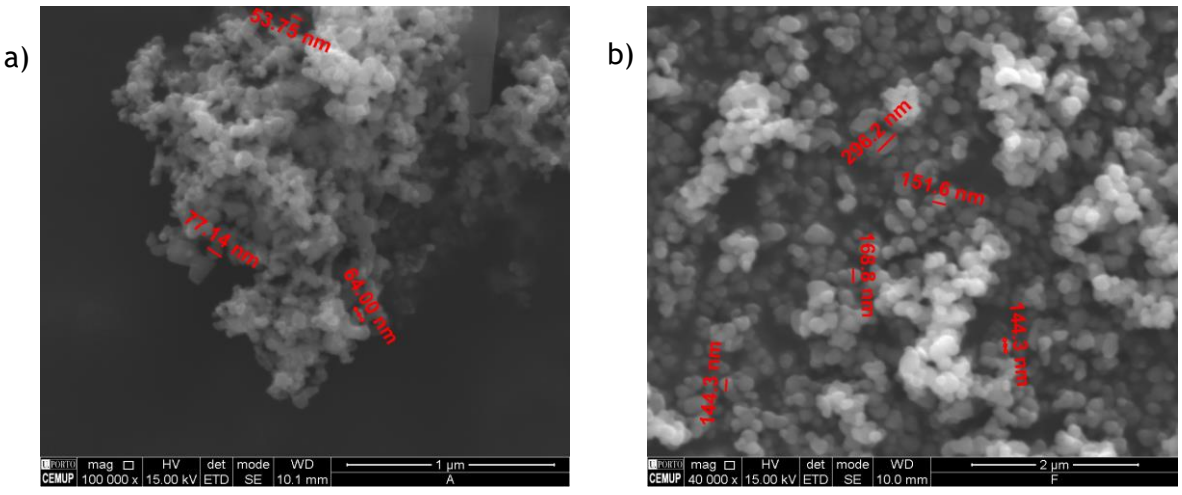

Figure 13: a) A and b) E particles SEM micrographs

Figure 14 represents the EDS spectra of a) B and b) C with their respective SEM: the B aluminosilicate composition and faujasite structure [45] and the several minerals composition and C showed the lamellae structure [46]. The small trace of titanium present in the Figure 14 is probably due to E leftovers in the extruder.

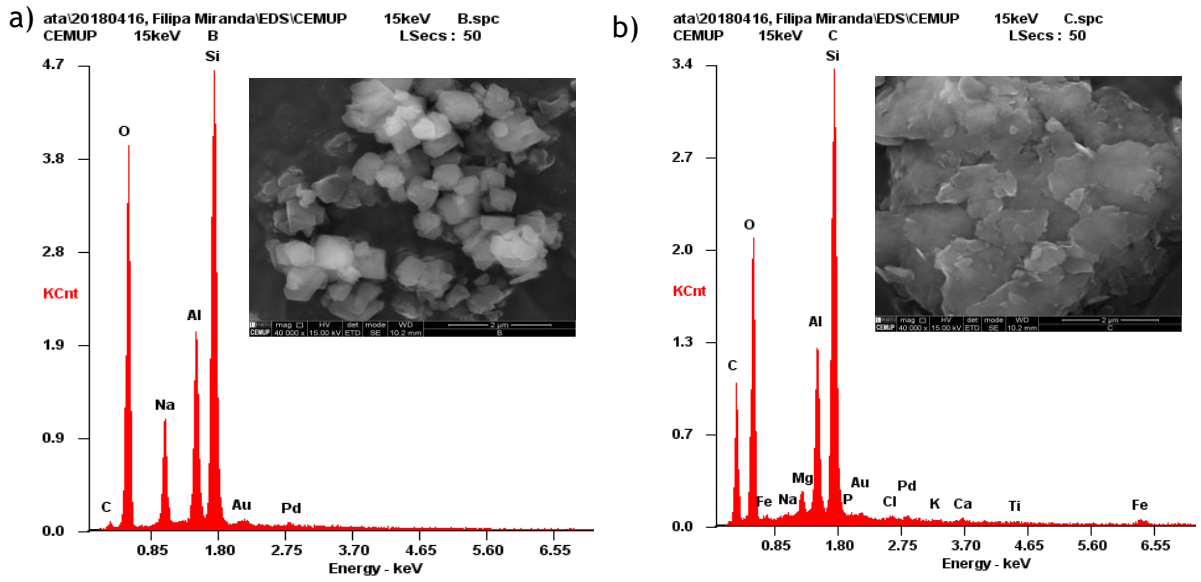

Figure 14: EDS Spectra and SEM micrographs of a) B and b) C

4.1.7 Temperature Programmed Desorption (TPD)

The TPD analysis was performed to evaluate the type of functionalized groups introduced into the catalysts surface and to quantify the amount of oxygen desorbed from the surface in form of CO and CO_2.

Table 3 presents the CO and CO_2 amounts of the A samples and the respective ratio of CO and CO_2. It is possible to observe a significant increase in the amount of desorbed CO and CO_2 after the functionalization. However, it was expected that the CO/CO_2 ratio would decrease as the main goal was to introduce acidic carboxylic groups. In fact, the amount of oxygen released as CO_2 is in both cases slightly higher than the amount released as CO, which means that oxygen functionalities with more acidic character were introduced in both functionalisation methods.

Table 3: Amounts of CO and CO released in the A samples and their ratio

Sample	CO (μmol·g^{-1})	CO_2 (μmol·g^{-1})	CO/CO_2
A	68.5	94.9	0.724
A Acid Treated	251	256	0.980
Δ (%)	265.8	169.7	36.1

In Figure 15, it is possible to observe which groups were introduced in the A Acid Treated sample: anhydrides, carbonyls, phenols and carboxylic groups [36]. Phenols temperature range overlaps with anhydrides and carbonyls in the CO spectra nevertheless this group is not expected after functionalization [34]. A small amount of lactones can be found in the CO_2

spectra. On the other hand, the pristine A showed some anhydrides apart from a very small amount of other unidentified groups. In addition, there is a sharp peak in the lower temperature region in CO_2 spectra which can be assigned to CO_2.

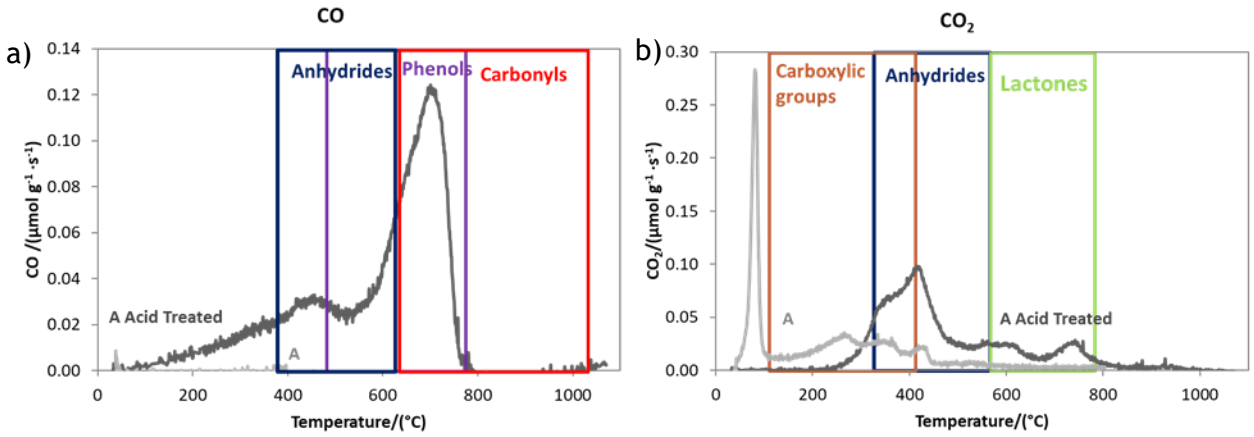

Figure 15: a) A and b) A Acid Treated TPD spectra with the functionalized groups

The TPD analysis was also performed for the F samples. Table 4 presents CO and CO_2 amounts, their ratio and the oxygen percentage. The observed increase in the release of CO and Co_2 in the F-Func is much higher than that registered in case of the A Acid Treated. The CO/CO_2 difference shows that no big changes occurred in acidity characteristic of F bulk samples.

Table 4: Amounts of CO and CO released in the F samples including their ratio and oxygen percentage

Sample	CO (µmol·g^{-1})	CO_2 (µmol·g^{-1})	CO/CO_2	O (%)
F	756	353	2.14	2.34
F-Func	4496	2006	2.24	13.6
Δ (%)	495	469	4.70	482

The Figure 16 confirms the inclusion of carboxylic groups, anhydrides and carbonyls as it was the liquid oxidation goal [36]. Phenols and lactones were also on the surface of F-Func.

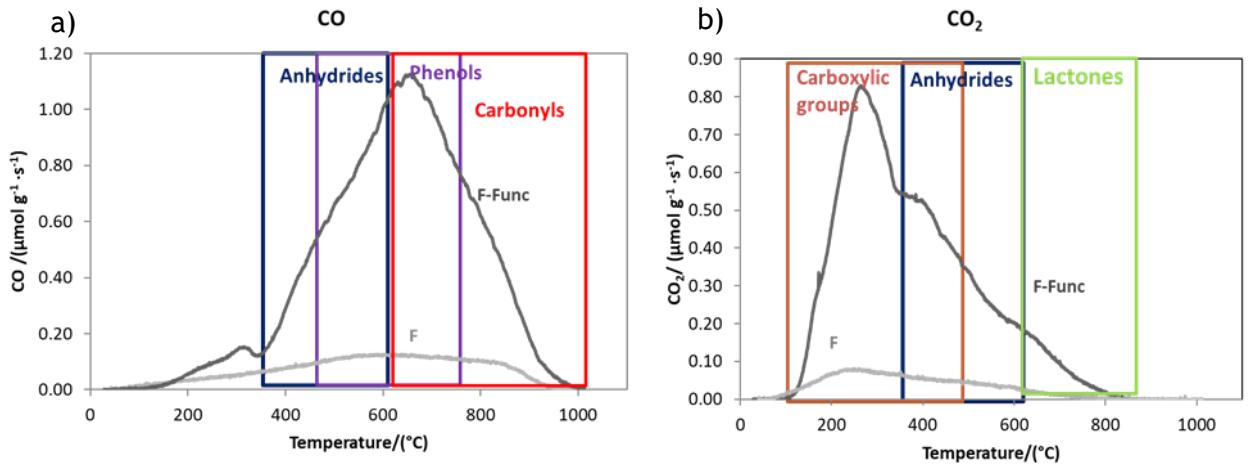

Figure 16: a) F and b) F-Func TPD spectra with the functionalized groups

4.1.8 Elemental Analysis (EA)

An elemental analysis was performed to quantify the chemical elements present in the F samples bulk [36].

Table 5 presents the results of the elemental analysis where is possible to observe that substantial changes occurred. The treatment with nitric acid let to some incorporation of nitrogen. Carbon percentage decreased as this element was oxygenated groups created on the surface of the F. There was significant increase of oxygen amount from 3.7 in the pristine F to 25 % after the functionalization.

Table 5: F samples elemental analysis

Sample	N (%)	C (%)	H (%)	O (%)
F	0.010	93	0.67	3.7
F-Func	0.67	72	1.8	25
Δ (%)	6600	-22	173	582

It is possible to compare both oxygen percentages from EA and TPD analysis. EA has higher values as this analysis is carried until 1450 ºC as TPD is only carried until 1050 ºC. It is noted that above 1050 ºC, oxygen can be further release. EA measurement also takes into account oxygen released not only in the of CO and CO_2 but also as water or as O_2.

4.2 Fibre Production

Some variations during samples preparation were observed. Those variations are presented and marked with arrows in Figure 17.

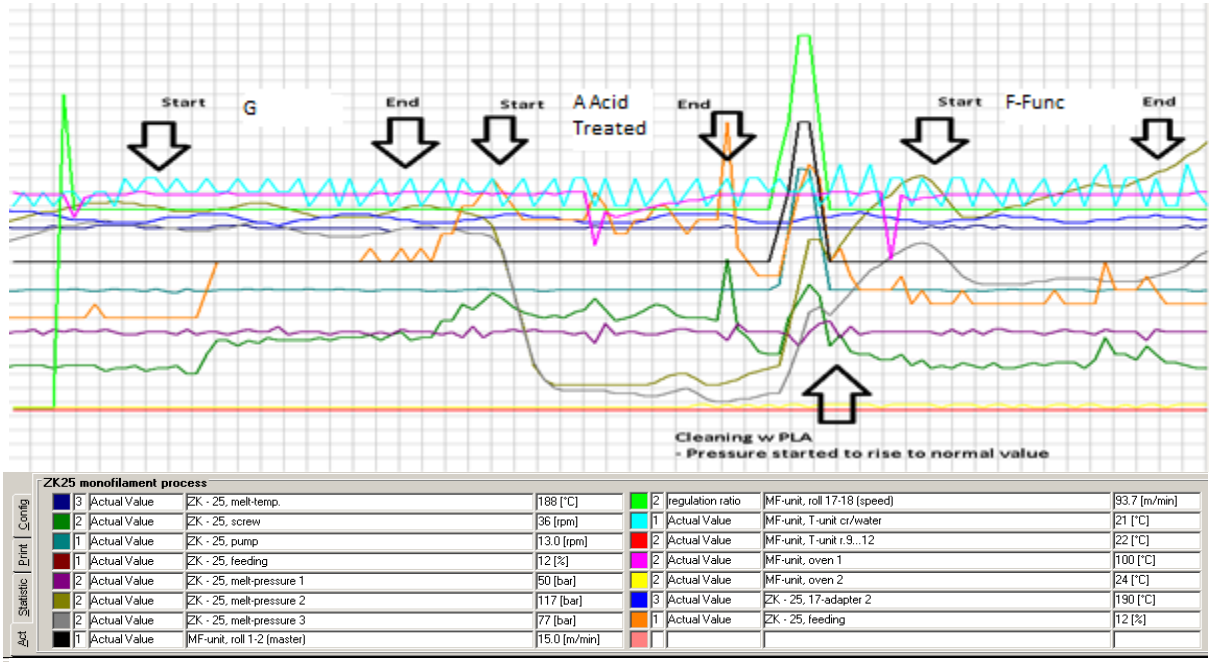

Figure 17: Overview of production conditions changes while A Acid Treated and F-Func fibres production

It was possible to observe constant melt pressure during G production. However, when the A + CA mixture was introduced in the hopper the melt pressure decreased drastically as soon as the mixture went into the extruder. This might be due to a very high activity of this treated catalyst that might have had resulted in the degradation of the polymer already inside the extruder. As a result, the fibre produced using this catalyst was not correctly produced so it was not included in testing. However, it was analysed by GPC and tensile tests were performed to try to understand the functionalization impact in this fibre on the properties of PLA.

Pristine PLA pellets were introduced in the hopper and it was possible to observe that the melt pressure started to rise to normal values. Then when the F-Func mixture was introduced the melt pressure did not stabilize during the process as the acid active groups on the F-Func could have onset the rapid degradation of the PLA pellets.

4.3 Hydrolysis tests

A control hydrolysis test at 70 ºC was performed in order to optimise the duration of the analysis. The pristine fibre was left shaking during 13 days (312 h) in the test bottles. After 7

days (168 h) some signs of early degradation were shown. pH (Appendix Figure 20), TOC (Appendix Figure 21) and TGA (Appendix Table 5: Thermogravimetric analysis of the hydrolysis test to verify the changes within positions 1 to 4: 312 h) in the Appendix 7, were performed to evaluate the pristine fibre behaviour and the water shaker conditions. Knowing that the catalysts activity should increase the reaction rate, the test with the catalysts was shorten to only 240 h (10 days). In addition, 10 days' time was previously to be sufficient time for the PLA fibre to start to degrade reported in [11].

Relating Appendix Table 4 with Appendix Table 5 (in the Appendix 7) it is possible to conclude that each position influences the samples in a different way, so it was decided to rotate the test flasks clockwise.

A test was performed at 70 ºC (This is because 70 ºC is the temperature of the composting thermophilic phase [6] and the catalyst should be active at this temperature.) Another test was carried out at 40 ºC (since this is close to the maximum temperature that might occur in the greenhouses, so catalyst should be inactive in these conditions).

4.3.1 pH

As a measurement of the water acidity due to the presence of carboxylic groups from the hydrolysis, pH was measured for the water samples withdrawn during hydrolysis reaction at 70 ºC and at 40 ºC. The higher activity of the catalyst was considered for the fibres with catalysts materials that showed lower pH value of the reaction water than that of the pristine PLA after 240 h. The lower value of pH was due to the presence of higher concentration of carboxylic groups in the reaction waters. As it was mentioned before, the carboxylic groups are the main product of hydrolytic degradation of PLA fibres. Two batches of the catalysts were studied 70 ºC and 40 ºC hydrolysis. They were considered as active catalysts the ones which presented lower pH than the pristine fibre after 240 h. Due to the number of samples, they were considered the testing had to be separated in two different batches. In both batches the benchmark PLA fibre was included to ensure the test reproducibility.

4.3.1.1 70 ºC

The Figure 18 shows the pH results from the 1st batch of the 70 ºC hydrolysis test. The pristine fibre has some amorphous parts which allow the water to diffuse and therefore showed differences in pH even without catalysts. High catalytic activity of A agrees well with the earlier reports from similar reaction under different testing conditions [28]. C and B were also found active, probably because as their structures swell when they are in contact with water giving it free space and increasing the diffusion rate [45] [46]. Although D is a carbon catalyst (which is chemically inert [47]) has a high mesoporous area which represents more free space for the water to diffuse explaining the lower pH than F. E has a very low surface area [29] and a crystalline structure [48] which gives a residual contact with the fibre and hinders water diffusion which explains the pH of the reaction water if PLA+E being higher than that of the pristine fibre. F has a lower mesoporous area then D [37]. Importantly, pH of the control water remained constant which means that there was no significant dissolution of CO_2 in the water.

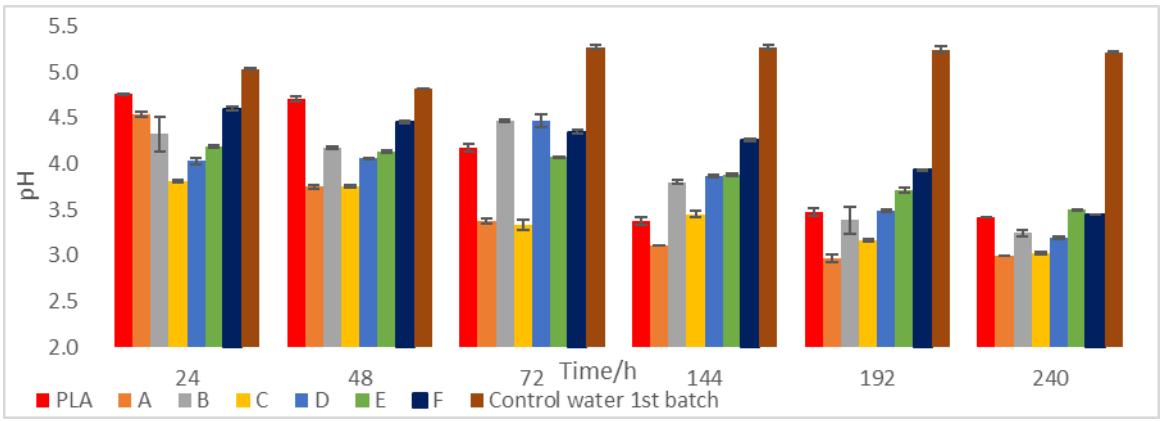

Figure 18: pH results from 1st batch of 70 ºC hydrolysis

Figure 19 shows the results from the 2nd batch including the pristine fibre duplicate. Polymer_A and Polymer_B did not show significant differences to the PLA pristine fibre probably because the added polymers are not miscible in the melt mixture with PLA when they are added in small percentages [50] [51]. Process_Aid showed nearly no difference to the pristine fibre pH which might indicate that the bond agent did not influence the reaction. G showed a small increase when compared to the pristine fibre probably due to the catalyst crystalline structure [49]. F-Func showed a marginal improvement relatively to F as the functionalization turned the catalyst into an active one due to its surface groups [37]. However, as the difference is not major it is possible that the edge hydroxyl groups formed hydrogen bonds and hindered the water diffusion [25] [27]. F-20 showed activity in the same range as F which might indicate that the pore distribution has no big influence in this case. However, the slight difference might be

due to the difference in textural properties has F-20 has small mesopore area and small pore volume than F. The control water pH variation is negligible.

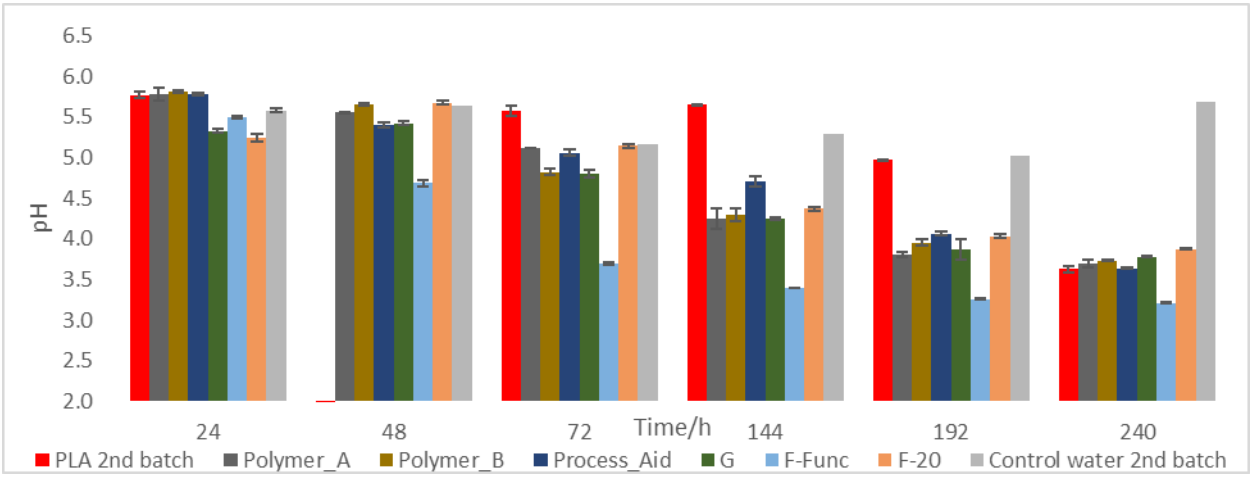

Figure 19: pH results from 2nd batch of 70 ºC hydrolysis

4.3.1.2 40 ºC

The 40 ºC hydrolysis test was performed with the 5 active catalysts from both batches. Figure 20 shows that the 5 catalysts are not active at 40 ºC which is the goal for this temperature.

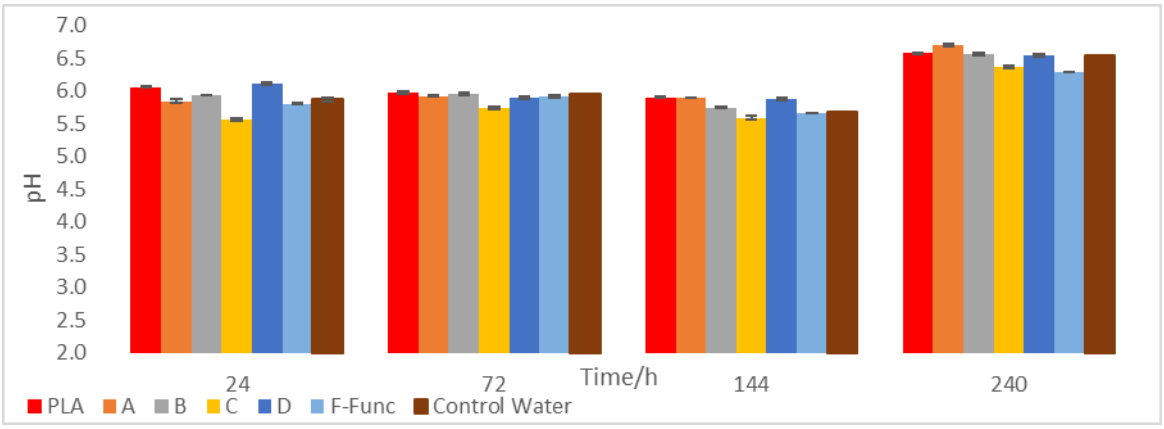

Figure 20: pH results from 40 ºC hydrolysis

4.3.2 Total Organic Carbon (TOC)

Total Organic Carbon measured mainly the carboxylic groups coming from hydrolysis but also other small compounds as CO_2 that might result from further hydrolysis. It is a complementary measurement to pH. They were considered as active catalysts the ones which presented higher TOC than the pristine fibre after 240 h.

4.3.2.1 70 ºC

Figure 21 shows the results from the 1st batch of 70 ºC hydrolysis. In 144 h and 192 h it was possible to notice a big increase in TOC values due to a contamination with organic solvent. The results corroborated well with pH results. Similarly, the A was shown to be the most active catalyst having the highest TOC and the lowest pH.

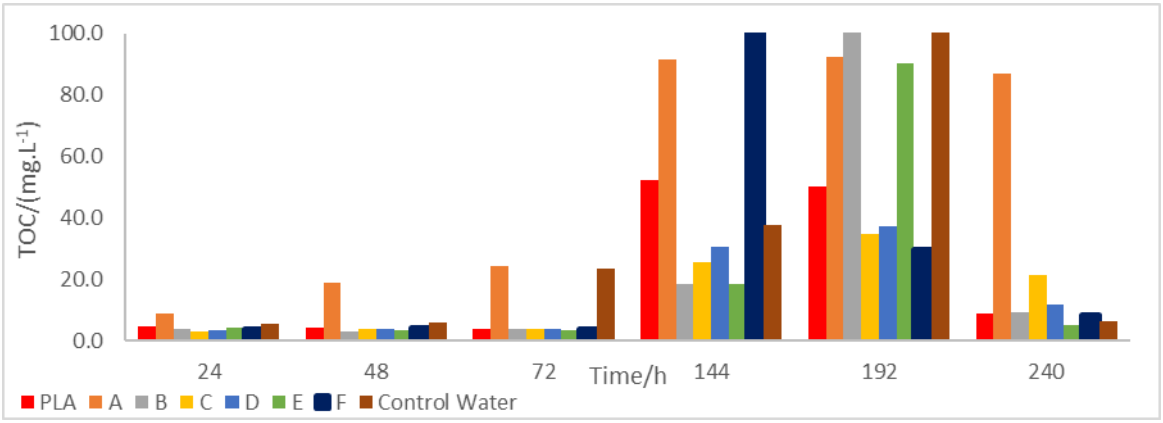

Figure 21: TOC results from 1st batch of 70 ºC hydrolysis

Moreover, D has a higher value than B (whereas D has a lower pH than B) probably because some catalyst particles might contribute to TOC themselves.

Figure 22 shows the results from the 2nd batch. It shows that the test is reproducible as the value for the PLA 2nd batch is very similar to the 1st batch. Polymer_A was previously reported to degrade in aquatic environments [31]. In fact, PLA+ Polymer_A was found to be less active than the PLA pristine fibre it might be degrading parts of the fibre. The water from PLA+ Polymer_B has a lower TOC value as it is a more crystalline polyester than PLA [33]. Process_Aid is reported to increase the mobility of macromolecular chains which promotes crystallinity explaining the lower TOC value than the pristine fibre. However it replaces intermolecular interactions between Process_Aid and PLA which are important for crystals formations which explains that the value is higher than the completely crystalline G [52]. G presented a very low TOC value when compared to the pristine fibre which agreed with the pH measurements. F-Func revealed an increase in the TOC value when compared with F. The functionalized catalyst was considered active as in in hydrolytic dehydration of PLA in agreement with the pH measurements.

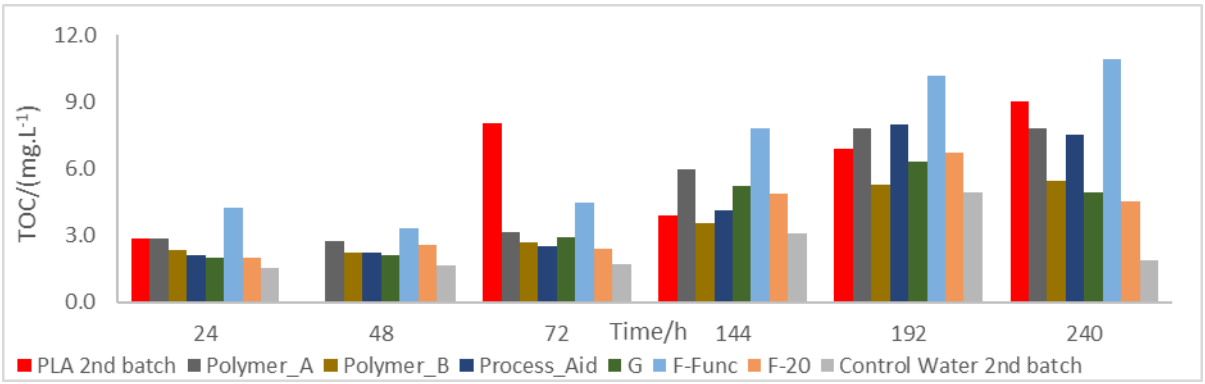

Figure 22: TOC results from 2nd batch of 70 ºC hydrolysis

In some of the catalysts TOC values, it was possible to observe an increase in TOC value to a maximum and then a decrease. This might happen as some groups are so small that become volatiles and evaporate leaving the water non saturated for new groups to dissolve.

4.3.2.2 40 ºC

The analysis the TOC of the water from the hydrolysis taking place at nearly 40 ºC confirmed the pH measurements as the TOC variations between the studied catalysts are nearly negligible.

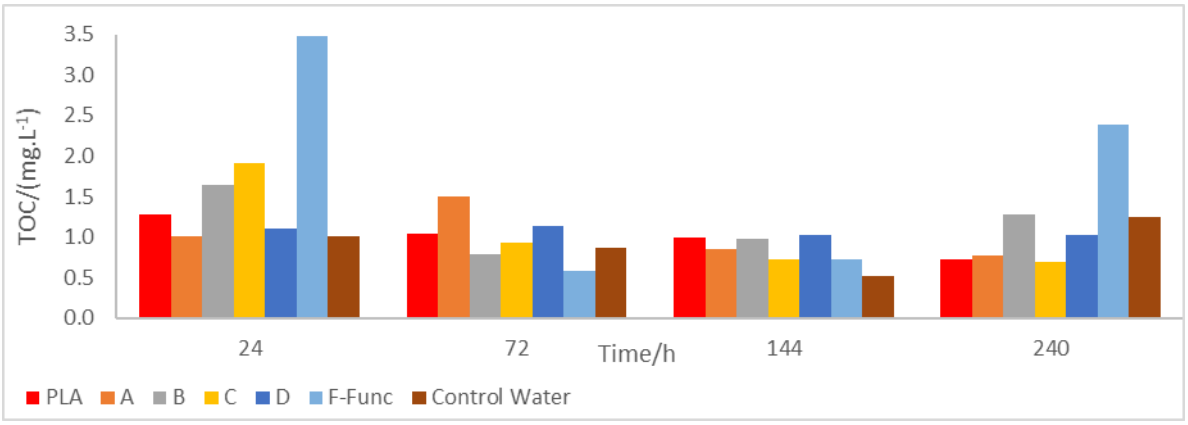

Figure 23: TOC results from 40 ºC hydrolysis

4.3.3 Gel Permeation Chromatography (GPC)

The fibres from the first batch of hydrolysis at 70 ºC were analysed by GPC. From these results it can be concluded that the GPC analysis was coherent with the pH and TOC results, presenting A as the most degraded fibre (as it has the lowest M_n and M_W values). B presents the highest M_n and M_W values which is according to the reported reinforcing mechanical properties given which are typical for the zeolites [45] [53].

Table 6: GPC data from 1st batch hydrolysis at 70 ºC for 240 h

240 h	PLA	A	B	C	D	E	F
M_n (g·mol^{-1})	7759	5107	11262	6719	8105	10281	9769
M_W (g·mol^{-1})	15114	10522	23300	12615	15835	21783	19947

4.3.4 Scanning Electron Microscopy with Energy Dispersive Spectroscopy (SEM/EDS)

PLA (Figure 24), A (Figure 25) and E (Figure 26) SEM micrographs are presented to compare the morphology with and without catalysts and before and after hydrolysis. These images are representative of the fibres aspect.

Figure 24 shows the difference between pristine PLA before and after hydrolysis which confirmed the degradation signs of the fibre after 10 days reaction, which is in line with the previous TOC and pH [11].

Figure 25 shows the clear difference of PLA+A fibre and PLA fibre as some signs of degradation are visible before hydrolysis. After hydrolysis, the A fibre is obviously degraded.

Figure 26 displays a different particle behaviour. No difference between pristine fibre and PLA + E could be noticed before hydrolysis and after 240 h. These images are agreeing with the reinforcing effect of E [29].

a) b)

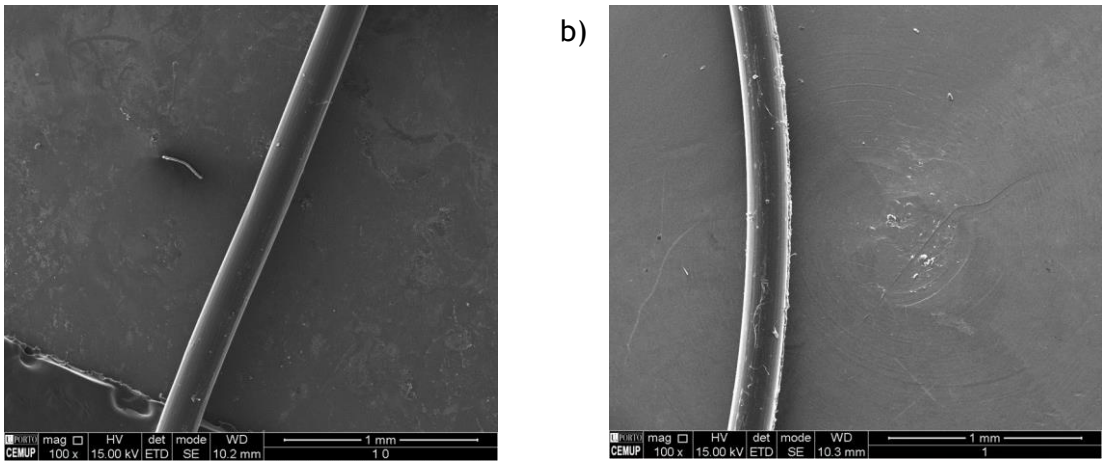

Figure 24: a) PLA before hydrolysis and b) PLA after 240 h 70 ºC hydrolysis

a) b)

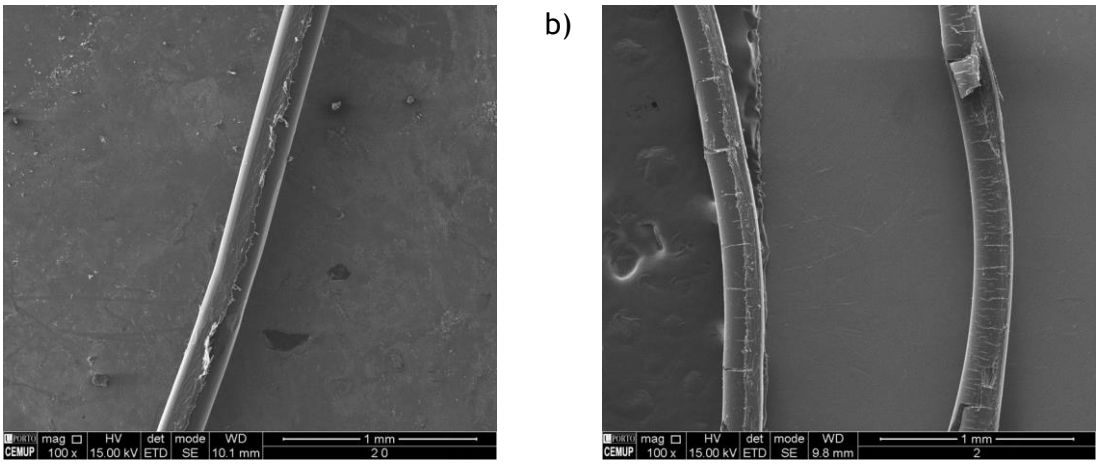

Figure 25: a) A before hydrolysis and b) A after 240 h 70 ºC hydrolysis

a) b)

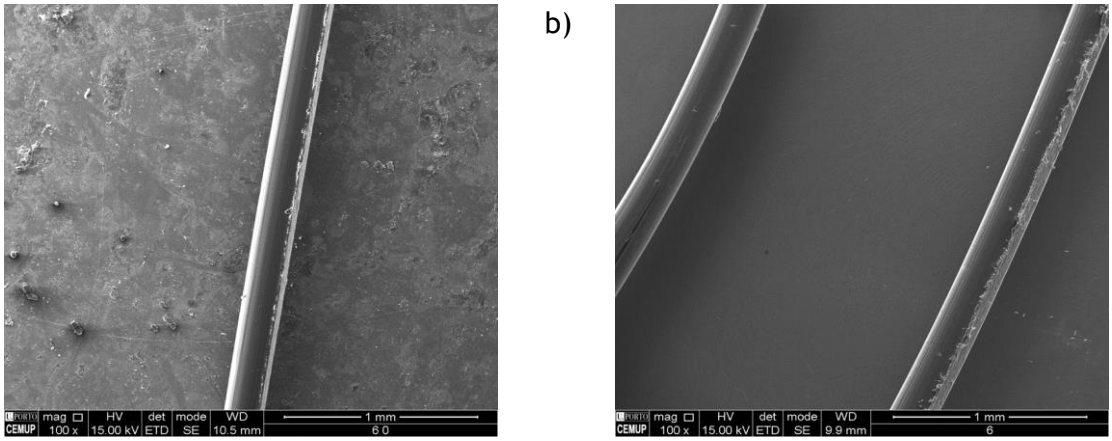

Figure 26: a) E before hydrolysis and b) E after 240 h 70 ºC hydrolysis

4.3.5 Thermogravimetric Analysis and Differential Scanning Calorimetry (TGA and DSC)

A thermogravimetric analysis was performed to evaluate the fibres behaviour in an inert atmosphere. However, no relevant results were obtained from the DSC analysis as it was not possible to include a cooling stage as the thermogravimetric analysis and the DSC analysis were performed at the same time. Priority was given to the thermogravimetric analysis.

Conclusions of this analysis are going to be based in T_{onset} and T_{peak} as these two are most reliable values since they are calculated automatically by the software.

All of the tables with the thermogravimetric results are presented in Appendix 9.

4.3.5.1 Before Hydrolysis Test

Appendix Table 6 presents the analysis before hydrolysis. All of the catalysts except the A had negligible differences when compared to the pristine fibre (T_{peak} -3 % < T_{peak} < T_{peak} + 2 %). The A due to its intense thermal degradation activity presented a decrease of 16 % on the T_{peak} which is a concern as the twine might degrade easily in work conditions [19] [28].

4.3.5.2 70 ºC

Appendix Table 7 resumes the data after 240 h of 70 ºC hydrolysis. Both pristine fibres (1st batch and 2nd batch) presented no relevant difference over the value before hydrolysis. Most of the fibres (PLA + catalysts) did not show relevant differences to the pristine fibres under the same conditions. PLA+G, PLA+Polymer_B, PLA+Process_Aid and PLA+A presented decreases higher than 5 % (6 %, 8 %, 13 % and 16 % respectively). G might have changed its properties and arrangement due to the hydrolysis effect as it was expected to induce thermal stability to PLA fibre [49]. Polymer_B might have decreased the thermal stability when compared to the pristine fibre as the mixture might did not have work [51] The Process_Aid intermolecular interactions with PLA fibre as already mentioned might have caused some disorder which decreased its thermal stability [52]. The A decrease agrees with the decrease presented before hydrolysis when compared to the pristine fibre [19] [28].

Polymer_B and Process_Aid showed important differences to the same fibres before hydrolysis: 9 % decrease for the polymer and 12 % for the bonding agent. Water might have contribute to weaken the already weak bonds between Polymer_B and PLA [51]. For the Process_Aid it might have happen that the water contributed to the disorder in the fibre and resulted in decreased thermal stability [52].

4.3.5.3 40 ºC

From Appendix Table 8, it is possible to observe that all the five chosen catalysts (PLA+A, PLA+B, PLA+C, PLA+D, PLA+F-Func) degraded thermally more than the pristine fibre. The pristine fibre presented no difference over the value before hydrolysis. However it can be considered that when compared to the pristine fibre the decrease in the T_{peak} of C and B is irrelevant as the difference to the pristine fibre is -3 % for the clay [54] and -5 % for the zeolite [53]. The A had a decrease of 18 % [19] [28] which is an issue as this temperature might be achieved in the greenhouses and this behaviour might lead to degradation of the twines.

When comparing the catalysts performance before and after 240 h in hydrolysis at 40 ºC it is possible to observe that the one which had a relevant change was the F-Func as the T_{peak}

decreased 14 % when compared to this parameter before hydrolysis. This value is also lower than that at the end of hydrolysis at 70 ºC.

4.4 Tensile tests

Tensile tests were performed to evaluate tenacity and elongation behaviour as the fibres were exposed to different conditions [44]. “Non treatment applied” refers to the fibre right after production. “After heat treatment” is reported to the heat treatment applied during 12h at 55 ºC in the lab oven.

The PLA pristine fibre results are presented in both Figure 27 and Figure 28 as goal lines as it is the standard. In optimal conditions the catalyst presence would improve the pristine PLA fibre conditions as an increase of mechanical properties is desired.

All of the catalysts and Polymer_A, Polymer_B [33] and Process_Aid [52] made the fibre weaker when compared to the pristine PLA fibre as all the bars are below the goal lines (Figure 27). Appendix Table 9 resumes the changes caused by the catalysts insertion where is possible to quantify the variations: E [29], Polymer_A [50], Polymer_B [33] present the lowest decreases in tenacity which can be considered negligible (> 10 %) as the addition of Process_Aid itself decreased the fibre tenacity in 10 %.

It is possible to observe in Figure 27 that pristine PLA fibre tenacity increased after heat treatment. The heat treatment should have transformed amorphous phase fibre parts into crystalline parts which made the fibre more resistant to the fracture as it is possible to observe also in Appendix Table 10 that all the fibres with the exception of A Acid Treated fibre increased theirs tenacities when compared to the same fibres before the heat treatment. When compared to the pristine fibre after heat treatment, only Polymer_B has a similar value to PLA. E and Polymer_A decreases are also considered irrelevant. E results are agreeing with the reported reinforcing effect on PLA fibre [29].

On the other hand, after hydrolysis the property decreases in all the fibres as the water molecules should be occupying the free spaces of the amorphous phase and then fading the interactions. Only F-Func stayed constant after this treatment as it is possible to also observe in Appendix Table 11 when compared to itself before hydrolysis. When compared to the pristine fibre, all the other fibres have decreased tenacity although in a very slightly way.

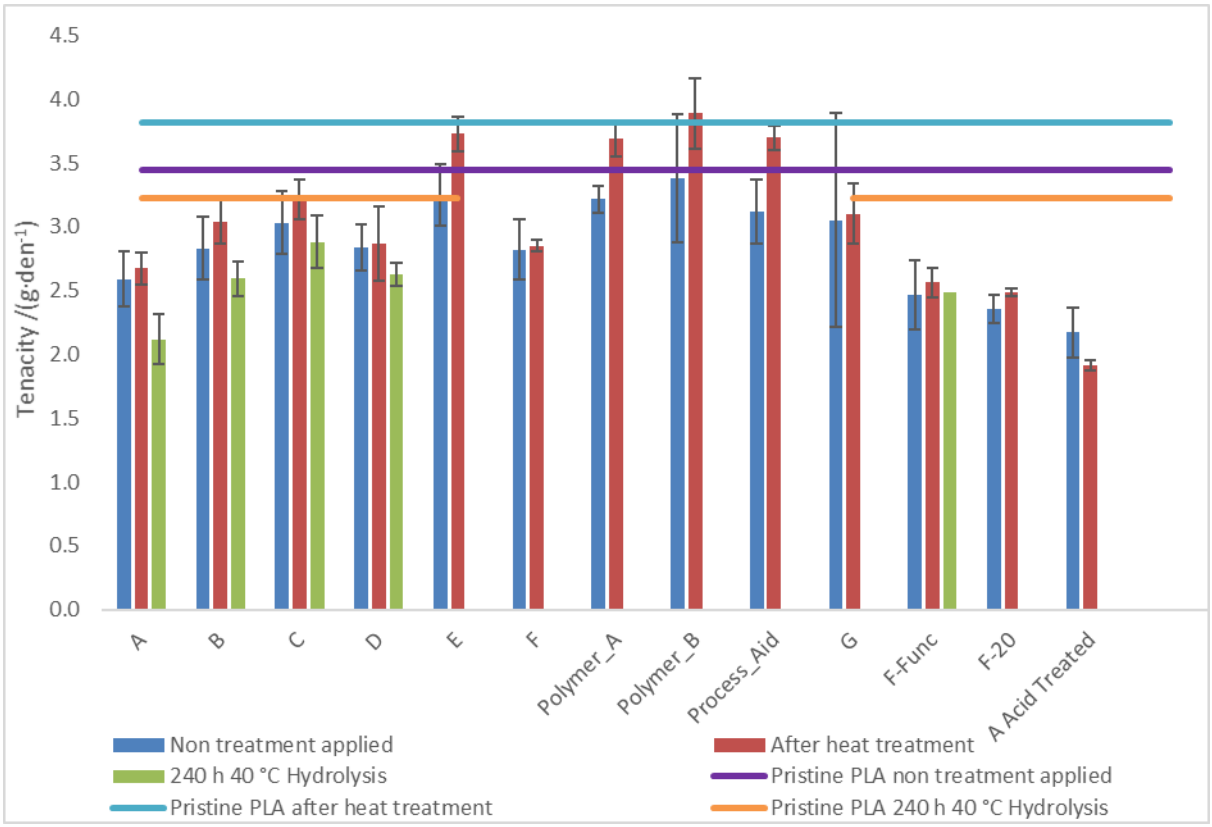

Figure 27: Fibres tenacity behaviour on the different conditions

Figure 27 shows that most of the catalysts and both polymers have higher elongation right after the production when compared to the pristine fibre. Only A Acid Treated, Process_Aid and F-20 have lower elongation than PLA fibre. The crystallinity characteristic of the Process_Aid addition might be the factor making the elongation decrease when compared to the pristine fibre [52]. F-20 presents the lowest decrease in elongation (-15 %) and C showed the biggest improvement (+24 %) [54]. These informations are resumed in Appendix Table 9.

Pristine PLA fibre elongation increases after heat treatment which can happen due to the molecules relaxation. C and Polymer_B had the only relevant increase in elongation when compared to the pristine fibre in the same conditions as actually it is reported [54] [33]. A, D and F showed no relevant changes when compared to themselves before the heat treatment and Process_Aid had the highest increase (> 30 %). After treatment elongation data is in Appendix Table 10.

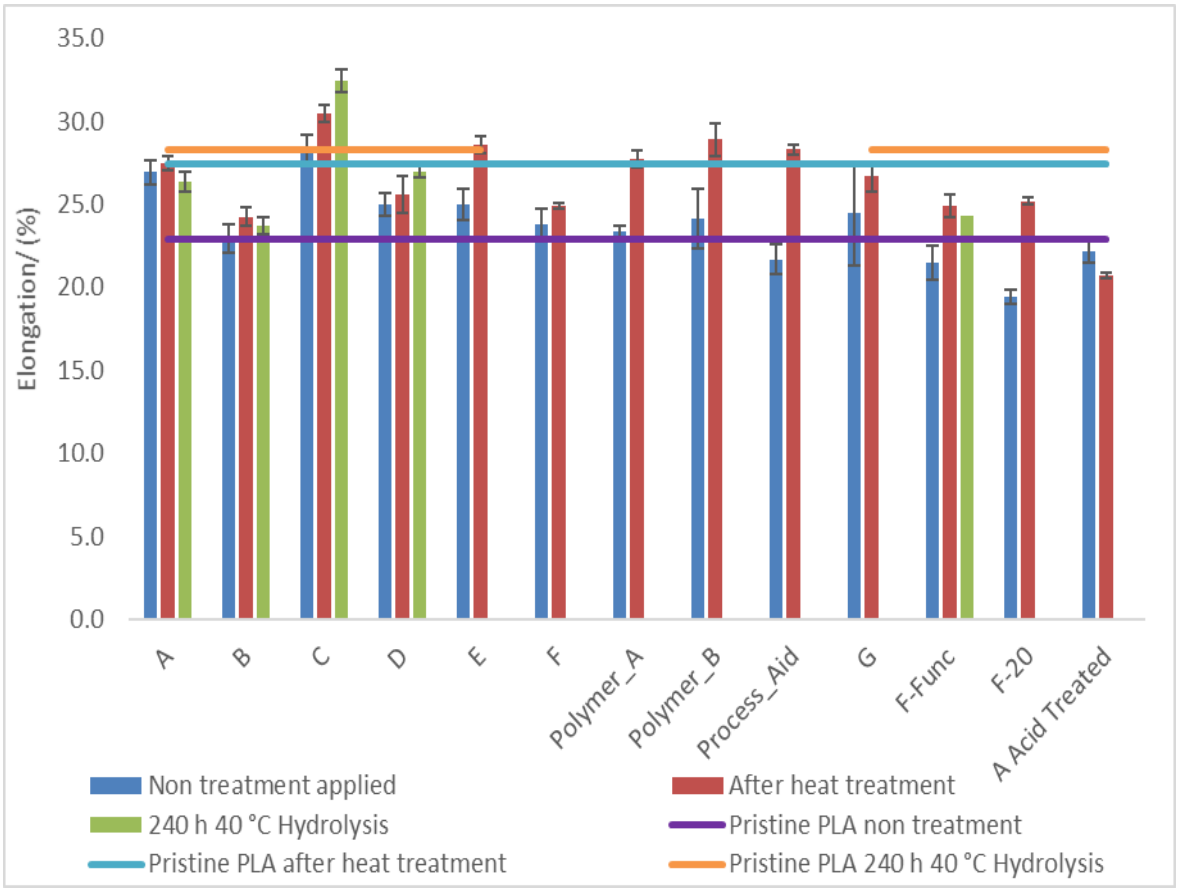

Figure 28: Fibres elongation behaviour on the different conditions

After hydrolysis, C shows a relevant increase in elongation (+14 %) and D shows a relevant decrease (-8 %) when compared to the same fibres before hydrolysis. Comparing with the pristine fibre, C still has a relevant increase (15 %) and all the other four catalysts shows decreases bigger or equal to 5 % being the B (-16 %) and the F-Func (-14 %) the most relevant decreases.

Due to its elongation tendencies in the different conditions and considering that the tenacity changes are irrelevant, C should be considered the catalyst that provides the best mechanical properties to the twines application [54].

5 Conclusion

Selected catalysts with varied surface chemistry, chemical composition and structure were characterized and then introduced in the fibres during extrusion process. The effect of the catalyst presence in the PLA fibre was tested under hydrolytic degradation and the resulting activity was compared on pH and TOC measurements of the reaction water and TG analysis of the fibres.

In order to improve the catalytic activity of A and F these materials were functionalized using citric and nitric acid. Changes were verified by TPD, EA and FT-IR.

A hydrolysis control test was performed to evaluate the time needed for the fibre to show signs of degradation and in order to optimise the set up conditions. The pristine PLA showed signs of degradation after 10 days. The control test involving only PLA, lasted 12 days, and the remaining tests, incorporating fibres with catalysts lasted 10 days. During the fibre production, it was verified that A Acid Treated was too active and the onset of PLA degradation was already observed on the PLA pellets inside the extruder. Similarly, F-Func also showed some signs of improved performance due to the decreased pressure of PLA melt. Nevertheless, it was possible to produce the fibre with F-Func.

Considering the composting process and the greenhouse temperatures two conditions were chosen for the tests: 70 ºC and 40 ºC. The most active catalysts at 70 ºC were A, C, B, D and F-Func, presenting the lower pH values, the higher TOC values and coherent results from GPC analysis. These catalysts proved not to be active at 40 ºC which is a requirement for the chosen catalyst due to the temperatures present in the greenhouses.

The analysis of the catalytic test made possible to conclude that the hydrolysis rate depends on the free space for water to diffuse. PLA itself degrades in water presence due to its semi-crystalline structure and its degradation being as self-catalytic reaction.

A presented a high catalytic activity due to the presence of hydroxyl groups on its surface. These groups attack the carboxylic groups from the PLA to form lactides or linear oligomers. However, it is necessary to control the –OH groups' amount as excessive –OH groups might create hydrogen bonds and then decrease the free space for water to diffuse.

C and B both have hydrophobic structures which swallow when they are in contact with water and the free space for the water to diffuse and react with the metallic particles of both catalysts.

Carbon catalysts as D are chemical inert. Mesopores provide the space needed for the water to diffuse and allow the particles to create bonds with the polymer. F-Func has a lower mesopore area than D however, it has oxygen groups in its surface which act as active centres.

Both E and G have crystalline structures. They are more organized so they have less space to the water to diffuse and less space to create new bonds with the PLA polymer which explains the reduced activity of these catalysts. They can be considered as reinforcing particles as they prevent PLA to hydrolyse and they improve the mechanical properties.

Polymer_A and Polymer_B did not show the expected results as probably the blending with PLA was not properly done. It should be considered an inclusion of an agglomerate agent. Process_Aid showed a slightly decrease in the fibre activity as it might have contributed to crystallinity increase.

The chosen catalyst can't accelerate thermal degradation of the fibre due to the greenhouse temperatures. Although they are not very high (and can also allow the fibres to improve their mechanical properties) the twines are going to be exposed there for months. The stocking period is also of concern since the twine should stay intact during this period.

The selected catalyst should not to decrease drastically the mechanical properties: a tenacity increase would be desirable for the product living time as it needs to support the weight of the fruits (e.g. tomatoes).

To choose the most suitable catalyst for hydrolytic degradation of PLA fibres in the composting conditions a reasonable combination between catalyst activity, thermal stability, mechanical properties, catalyst price and reproducibility under industrial conditions should be achieved.

Although A is by far the most active catalyst, it shows a relevant thermal stability decrease as well as a decrease in mechanical properties that would make the twines inoperative. It is not expensive and easy to reproduce to industrial conditions, generally recognized as safe and food contact approved by Food and Drug Administration.

C reunites the best set of properties: good catalytic activity, no changes in thermal stability and provided a relevant improvement in elongation. It is not expensive and is generally recognized as safe and food contact approved. On the other hand, it is not easy to reproduce the industrial conditions for keeping the same composition of the material and even small changes in each product batch can have a significant effect on its catalytic behaviour. Nevertheless, C should be a first option material considered for application in this project.

6 Assessment of the work done

6.1 Objectives Achieved

Selected catalysts with varied surface chemistry, chemical composition and structure were characterized and then introduced into the fibres. The effect of the catalyst presence in the fibre was tested under hydrolytic degradation conditions and it was possible to degrade more fibre within the same period of time after adding catalyst so the main goal of the work was achieved.

6.2 Limitations and Future Work

A limitation found during this work was the location of the water shaker bath. However, it was possible to state a temperature automatically for the water bath this equipment was placed in a room full of other equipment which dissipate a relevant quantity of heat and next to a window which might have had influenced the temperature during the hydrolysis tests.

The DSC analysis was also a limitation since a lot of the explanations for the results are based in the polymer/catalyst crystallinity and it was not possible to determine it experimentally as it was needed to include a cooling stage in the analysis to get reliable results. This stage would prevent the thermogravimetric analysis which was given priority due to the thermal degradation in the greenhouse.

Several catalysts were excluded from this study, including other clay, due to their particle size distributions results. As it is known that the suspensions were not correctly made it would be adequate to remeasure and verify if the results fit the extruder filter parameter.

A Acid Treated was proved to be a very active catalyst but it was not possible to test its effect on hydrolysis. It could be interesting to decrease the amount of this catalyst included in fibre to study its effects or reduce the citric acid concentration in the treatment.

The F was functionalized and showed some improvements. The liquid phase functionalization was hard to achieve so a gas phase could be tested also to verify the effect of other surface groups in the hydrolysis. D could also be functionalized as it presents a high mesopore area which could be an important parameter to water diffusion in hydrolysis.

Work is needed to be done to verify the economic viability of the chosen catalysts in industrial scale.

References

1. Euronete, "About Us: Royal Lankhorst Euronete Group bv," 2018. [Online]. Available: http://www.euronete.com/about_us/Royal_Lankhorst_Euronete_Group_bv. [Accessed 19 March 2018].
2. Euronete, "About Us: History," 2018. [Online]. Available: http://www.euronete.com/about_us/history. [Accessed 19 March 2018].
3. Euronete, "About Us," 2018. [Online]. Available: http://www.euronete.com/about_us/. [Accessed 19 March 2018].
4. Royal Lankhorst Euronete Group BV, *Case study 2: PLA compostable Bio-twine,* 2011.
5. M. Peet and G. Welles, "Greenhouse Tomato Production," in *Tomatoes*, The Netherlands, CAB International (ed. E. Heuvelink), 2005, pp. 257-304.
6. G. Felton, *Session 2: Fundamentals of the Composting Process,* USA: US Composting Council.
7. M. Karamanlioglu, R. Preziosi and G. D. Robson, "Abiotic and biotic environmental degradation of the bioplastic polymer poly(lactic acid): A review," *Polymer Degradation and Stability,* vol. 137, pp. 122-130, 2017.
8. E. Castro-Aguirre, F. Iñiguez-Franco, H. Sam sudin, X. Fang and R. Auras, "Poly(lactic acid)—Mass production, processing, industrial applications, and end of life," *Advanced Drug Delivery Reviews,* vol. 107, pp. 333-366, 2016.
9. R. Iovino, R. Zullo, M. Rao, L. Cassar and L. Gianfreda, "Biodegradation of poly(lactic acid)/starch/coir biocomposites under controlled composting conditions," *Polymer Degradation and Stability,* vol. 93, pp. 147-157, 2008.
10. M. Agarwal, K. W. Koelling and J. J. Chalmers, "Characterization of the Degradation of Polylactic Acid Polymer in a Solid Substrate Environment," *Biotechnol. Prog.,* vol. 14 No. 3, pp. 517-526, 1998.
11. J. Mofokeng, A. Luyt, T. Tábi and J. Kovács, "Comparison of injection moulded, natural fibre-reinforced composites with PP and PLA as matrices," *Journal of Thermoplastic Composite Materials,* vol. 25 No. 8, pp. 927-948, 2011.

12. C. B. Lin, “High polymer prices make PLA an attractive alternative - NatureWorks,” ICIS News, 20 May 2011. [Online]. Available: https://www.icis.com/resources/news/2011/05/20/9462068/high-polymer-prices-make-pla-an-attractive-alternative-natureworks/. [Accessed 6 June 2018].

13. Wikipedia, “Polylactic acid,” Wikipedia, 23 May 2018. [Online]. Available: https://en.wikipedia.org/wiki/Polylactic_acid. [Accessed 6 June 2018].

14. M. Jamshidh, E. A. Tehrany, M. Imran, M. Jacquot and S. Desobry, “Poly-Lactic Acid: Production, Applications, Nanocomposites, and Release Studies,” *Comprehensive Reviews in Food Science and Food Safety,* vol. 9, pp. 552-571, 2010.

15. Simagroup R&D Department, Thermoplastic Resins Fibers, Italy: L'Artiere Edizionitalia, 1998.

16. G. L. Siparsky, K. J. Voorhees and F. Miao, “Hydrolysis of Polylactic Acid (PLA) and Polycaprolactone,” *Journal of Environmental Polymer Degradation (PCL) in Aqueous Acetonitrile Solutions: Autocatalysis,* vol. 6, pp. 31-41, 1998.

17. K. Tomita, H. Tsujib, T. Nakajima, Y. Kikuchi, K. Ikarashib and N. Ikeda, “Degradation of poly(d-lactic acid) by a thermophile,” *Polymer Degradation and Stability,* vol. 81, pp. 167-171, 2003.

18. X. Qi, Y. Ren and X. Wang, “New advances in the biodegradation of Poly(lactic) acid,” *International Biodeterioration & Biodegradation,* vol. 117, pp. 215-223, 2017.

19. H. Abe, N. Takahashi, K. J. Kim, M. Mochizuki and Y. Doi, “Thermal Degradation Processes of End-Capped Poly(L-lactide)s in the Presence and Absence of Residual A Catalyst,” *Biomacromolecules,* vol. 5, pp. 1606-1614, 2004.

20. Hitachi High-Tech Science Corporation, *Thermal analysis of polylactic acid: Crystallinity and heat resistance,* Tokyo, Japan: Hitachi High-Tech Science Corporation, 2007.

21. D. A. McNaught and A. Wilkinson, IUPAC Compendium of Chemical Terminology, Cambridge, UK: Wiley-Blackwell; 2nd Revised edition, 1997.

22. H. S. Fogler, “Chap.10 Catalysis and Catalytic Reactors,” in *Elements of Chemical Reaction Engineering*, New Delhi, India, Prentice-Hall of India, Third Edition, 2004, pp. 581-603.

23. I. Fechete, Y. Wang and J. C. Védrine, “The past, present and future of heterogeneous catalysis,” *Catalysis Today,* vol. 189, pp. 2-27, 2012.

24. A. J. Dumesic, G. W. Huber and M. Boudart, “Ch 1. Principles of Heterogeneous Catalysis,” in *Handbook of Heterogeneous Catalysis*, Germany, Wiley-VCH Verlag GmbH & Co. KGaA., 2008, pp. 1-14.

25. H. Tsuji and T. Hayashi, “Hydrolytic degradation of linear 2-arm and branched 4-arm poly(DL-lactide)s: Effects of branching and terminal hydroxyl groups,” *Polymer Degradation and Stability,* vol. 102, pp. 59-66, 2014.

26. F. Iñiguez-Franco, R. Auras, J. Ahmed, S. Selke, M. Rubino, K. Dolan and H. Soto-Valdez, “Control of hydrolytic degradation of Poly(lactic acid) by incorporation of chain extender: From bulk to surface erosion,” *Polymer Testing,* vol. 67, pp. 190-196, 2018.

27. F. Iñiguez-Franco, R. Auras, M. Rubino, K. Dolan, H. Soto-Valdez and S. Selke, “Effect of nanoparticles on the hydrolytic degradation of PLA-nanocomposites by water-ethanol solutions,” *Polymer Degradation and Stability,* vol. 146, pp. 287-297, 2017.

28. E. Lizundia, L. Ruiz-Rubio, J. L. Vilas and L. M. Léon, “Towards the development of eco-friendly disposable polymers: A-initiated thermal and hydrolytic degradation in poly(L-lactide)/A nanocomposites,” *Royal Society of Chemistry,* vol. 6, pp. 15660-15669, 2016.

29. M.-X. Li, S.-H. Kim, S.-W. Choi, K. Goda and W.-I. Lee, “Effect of reinforcing particles on hydrolytic degradation behavior of poly (lactic acid) composites,” *Composites Part B,* vol. 96, pp. 248-254, 2016.

30. P. Stloukal, S. Pekarová, A. Kalendova, H. Mattausch, S. Laske, C. Holzer, L. Chitu, S. Bodner, G. Maier, M. Slouf and M. Koutny, “Kinetics and mechanism of the biodegradation of PLA/clay nanocomposites during thermophilic phase of composting process,” *Waste Management,* vol. 42, pp. 31-40, 2015.

31. E. Bugnicourt, P. Cinelli and V. Alvarez, “ Polymer_A: Review of synthesis,characteristics, processing and potential applications in packaging,” *eXPRESS Polymer Letters,* Vols. 8, No 11, p. 791–808, 2014.

32. European Bioplastics e.V., “Harmonised standards for bioplastics,” European Bioplastics, [Online]. Available: https://www.european-bioplastics.org/bioplastics/standards/. [Accessed 20 April 2018].

33. SUCCINITY GMBH, “Biobased Polymer_B – An attractive polymer for biopolymer compounds,” [Online]. Available: http://www.succinity.com/images/succinity_broschure.pdf. [Accessed 20 April 2018].

34. S. Mallakpour and N. Nouruzi, “Effects of citric acid-functionalized A nanoparticles on the structural, mechanical, thermal and optical properties of polycaprolactone nanocomposite films,” *Materials Chemistry and Physics,* vol. 197, pp. 129-137, 2017.

35. Y.-B. Huang and Y. Fu, “Hydrolysis of cellulose to glucose by solid acid catalysts,” *Green Chemistry,* vol. 15, pp. 1095-1111 , 2013.

36. J. L. Figueiredo, M. Pereira, M. Freitas and J. Órfão, “Modification of the surface chemistry of activated carbons,” *Carbon,* vol. 37, pp. 1379-1389, 1999.

37. A. M. Silva, B. F. Machado, J. L. Figueiredo and J. L. Faria, “Controlling the surface chemistry of carbon Fs using HNO3-hydrothermal oxidation,” *Carbon,* vol. 47, pp. 1670-1679, 2009.

38. Beckman Coulter Inc., “LS™ 200,” Beckman Coulter Inc., 2018. [Online]. Available: https://www.beckmancoulter.com/wsrportal/wsr/industrial/products/laser-diffraction-particle-size-analyzers/ls-200-series/index.htm#2/10//0/25/1/0/asc/2/6605209///0/1//0/ %2Fwsrportal %2Fwsr %2Findustrial %2Fproducts %2Flaser-diffraction-particle-size-analyzers. [Accessed 27 April 2018].

39. S. Swapp, “Scanning Electron Microscopy (SEM),” Science Education Resource Center: Carleton College, 26 May 2017. [Online]. Available: https://serc.carleton.edu/research_education/geochemsheets/techniques/SEM.html. [Accessed 2018 June 18].

40. J. Goodge, “Energy-Dispersive X-Ray Spectroscopy (EDS),” Science Education Resource Center: Carleton College, 26 April 2017. [Online]. Available: https://serc.carleton.edu/research_education/geochemsheets/eds.html. [Accessed 18 June 2018].

41. J. L. Figueiredo, M. F. R. Pereira, M. M. A. Freitas and J. J. M. Órfão, “Characterization of Active Sites on Carbon Catalysts,” *Industrial & Engineering Chemistry Research,* vol. 46, pp. 4110-4115, 2007.

42. I. Bisutti, I. Hilke and M. Raesslee, “Determination of total organic carbon – an overview of current methods,” *TrAC Trends in Analytical Chemistry,* vol. 23, pp. 716-726, 2004.

43. Agilent Technologies Inc., *An Introduction to Gel Permeation Chromatography and Size Exclusion Chromatography,* USA: Agilent Technologies Inc., 2015.

44. W. D. Callister, Jr., Materials Science and Engineering: An Introduction, USA: John Wiley & Sons, Inc. 7th Edition, 2007.

45. W. Lutz, "Zeolite Y: Synthesis, Modification, and Properties—A Case Revisited," *Hindawi Publishing Corporation,* pp. 1-20, 2014.

46. M. S. Nazir, M. H. M. Kassim, L. Mohapatra, M. A. Gilani, M. R. Raza and K. Majeed, "Characteristic Properties of Nanoclays and Characterization of Nanoparticulates and Nanocomposites," in *Nanoclay Reinforced Polymer Composites*, vol. XII, Singapore, Springer Science+Business Media, 2016, pp. 35-55.

47. F. Rodriguez-Reinoso, "The Role of Carbon Materials in Heterogeneous Catalysis," *Carbon,* vol. 36 No.3, pp. 159-175, 1998.

48. C. Marinescu, A. Sofronia, C. Rusti, R. Piticescu, V. Badilita, E. Vasile, R. Baies and S. Tanasescu, "DSC Investigation of Nanocrystalline E Powder," *Journal of Thermal Analysis and Calorimetry,* vol. 103, pp. 49-57, 2011.

49. C. Nico, T. Monteiro and M. Graça, "G oxides and G physical properties: Review and prospects," *Progress in Materials Science,* vol. 80, pp. 1-37, 2016.

50. T. Gérard and T. Budtova, "PLA-Polymer_A blends: morphology, thermal and mechanical properties," in *International Conference on Biodegradable and Biobased Polymers - BIOPOL 2011*, Strasbourg, France, 2011.

51. G.-X. Chen, H.-S. Kim, E.-S. Kim and J.-S. Yoon, "Compatibilization-like effect of reactive organoclay on the poly(l-lactide)/poly(butylene succinate) blends," *Polymer,* vol. 46, pp. 11829-11836, 2005.

52. M. K. Fehri, C. Mugoni, P. Cinelli, I. Anguillesi, M. B. Coltelli, S. Fiori, M. Montorsi and A. Lazzeri, "Composition dependence of the synergistic effect of nucleating agent and plasticizer in poly(lactic acid): A Mixture Design study," *eXPRESS Polymer Letters,* vol. 10 No. 4, pp. 274-288, 2016.

53. A. Lopes, P. Martins and S. Lanceros-Mendez, "Aluminosilicate and aluminosilicate based polymer composites: Present status, applications and future trends," *Progress in Surface Science,* vol. 89, pp. 239-277, 2014.

54. S. Joseph and W. W. Focke, *Poly (Ethylene-vinyl co-vinyl acetate) /Clay nanocomposites: mechanical, morphology and thermal behavior,* Institute of Applied Materials, Department of Chemistry and Chemical Engineering: Lynwood Road, South Africa.

Appendix 1 Manufacturing process of Poly(lactic acid)

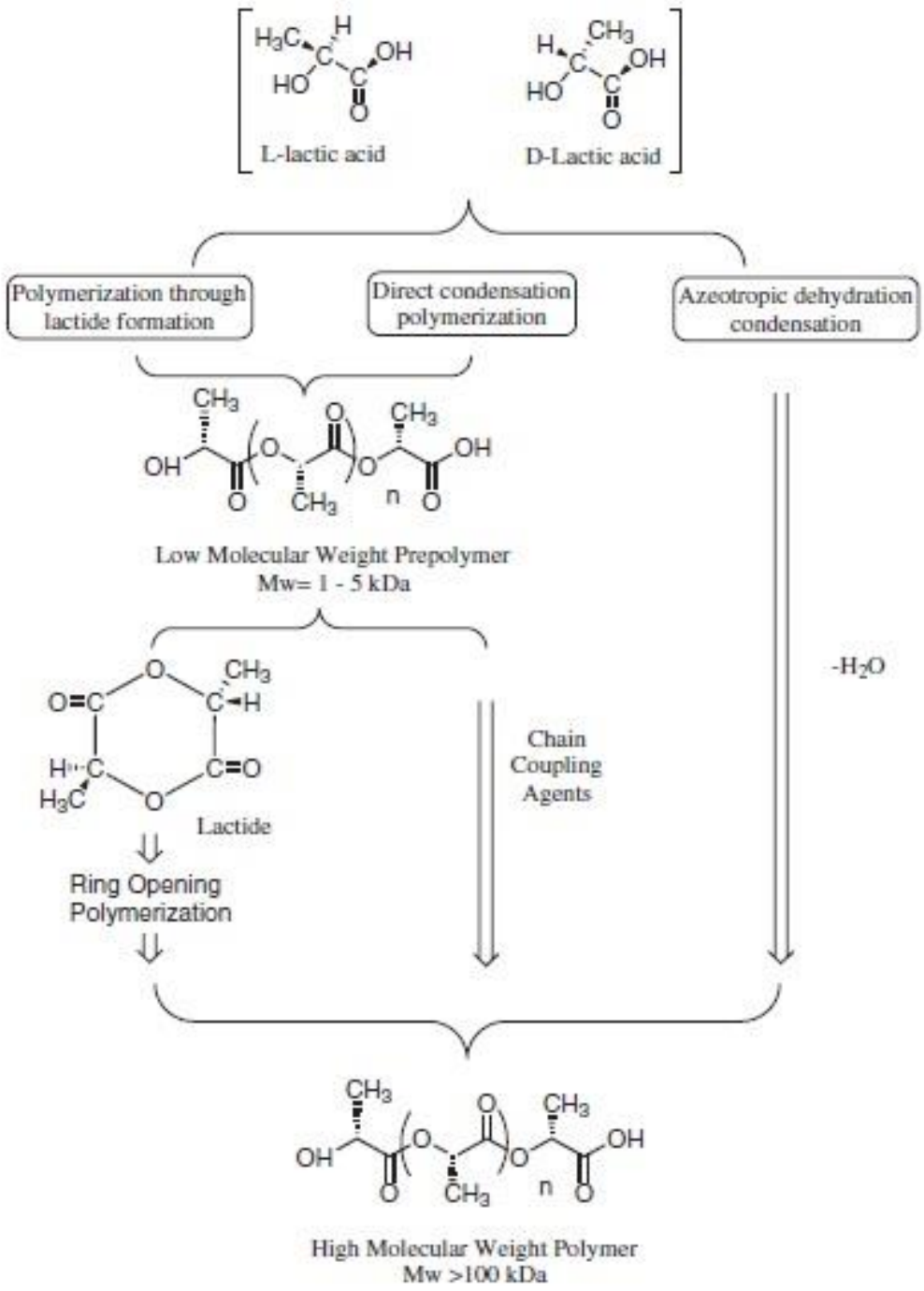

Appendix Figure 1: Poly(lactic acid) manufacturing processes

Appendix 2 PLA Degradation microorganisms

Appendix Table 1: PLA degradation microorganisms and enzymes families

Actinomycetes	**Bacteria**	**Fungus**	**Enzymes**
Amycolatopsis	*Bacillus*	Tritirachium	Proteases
Saccharothrix	*Pseudomonas*	Cryptococcus	Lipases
Kibdelosporangium	*Stenotrophomonas*	Aspergillus	Cutinases
Actinomadura	*Alcanivorax*	Trichoderma	Esterases
Laceyella	*Alcaligenes*		
Pseudonocardia			

Appendix 3 Fibre production

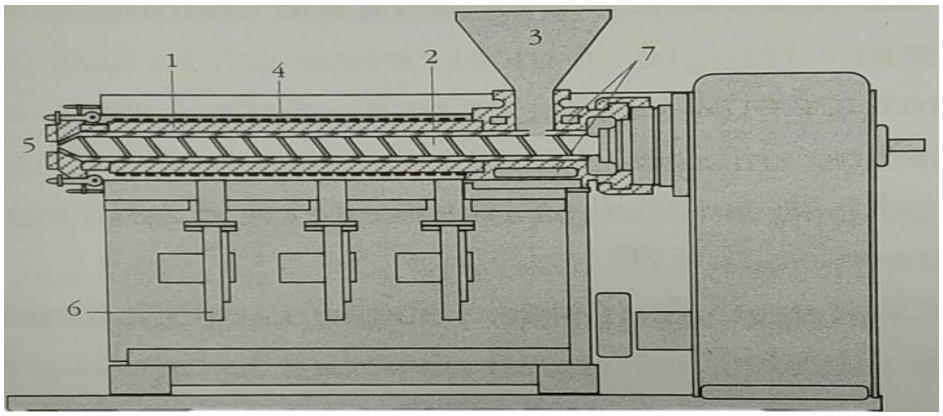

Appendix Figure 2: Single-screw extruder: 1. Cylinder; 2. Screw; 3. Hopper;4. Heating elements; 5. Terminal opening for resin outlet; 6. Cooling fans; 7. Channel for cooling liquid of feed beginning

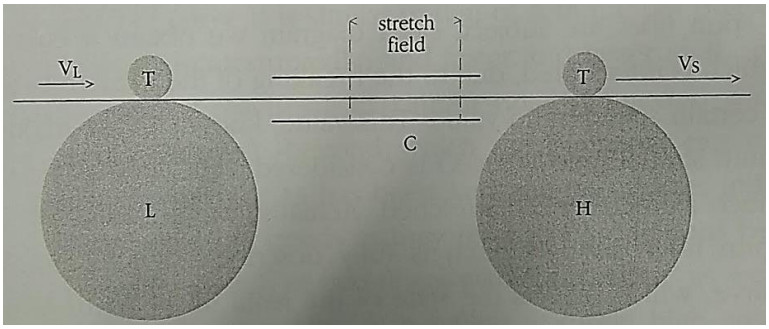

Appendix Figure 3: Stretch stage outline

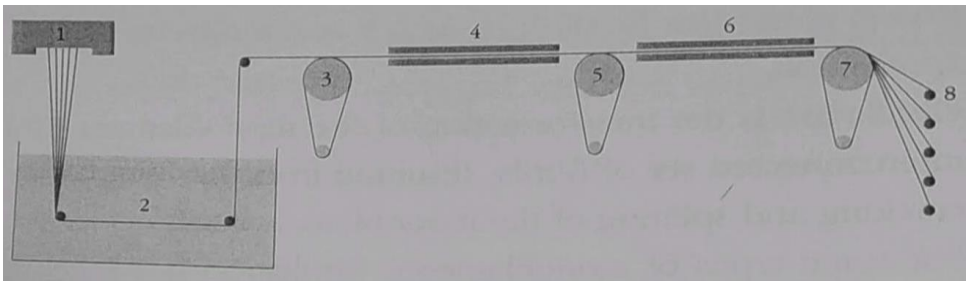

Appendix Figure 4: Monofilaments process after extrusion stage

Appendix 4 Catalysts Particle size distribution comparison: suspension and ball milling

"Water" stands for non-milled samples measured in a water suspension and "US" stands for non-milled samples measured in an ethanol suspension after 15 min ultra-sonication. Only B, C and J went through ball-milling process. B and J milled samples were measured in ethanol suspension, C was measured in propanol suspension and all of them were sonicated for 15 min. The milling time and frequency are presented in the corresponding graphs curves.

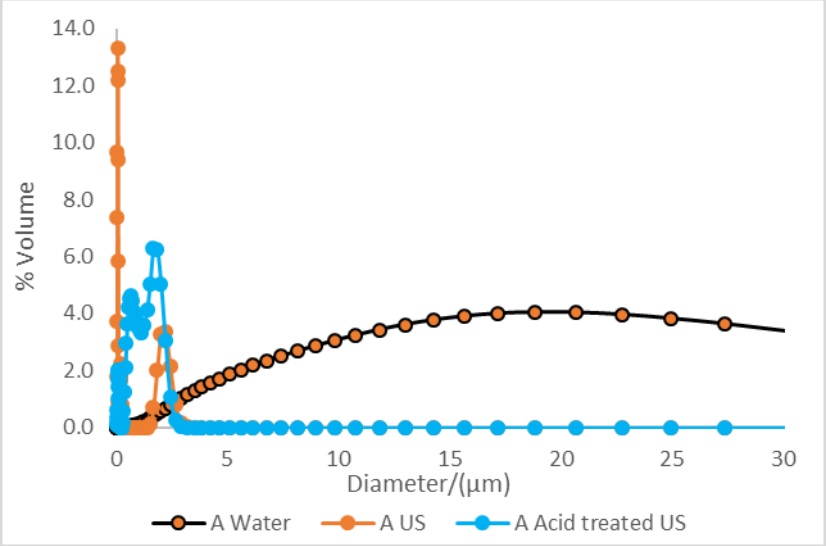

Appendix Figure 5: A particle size distribution

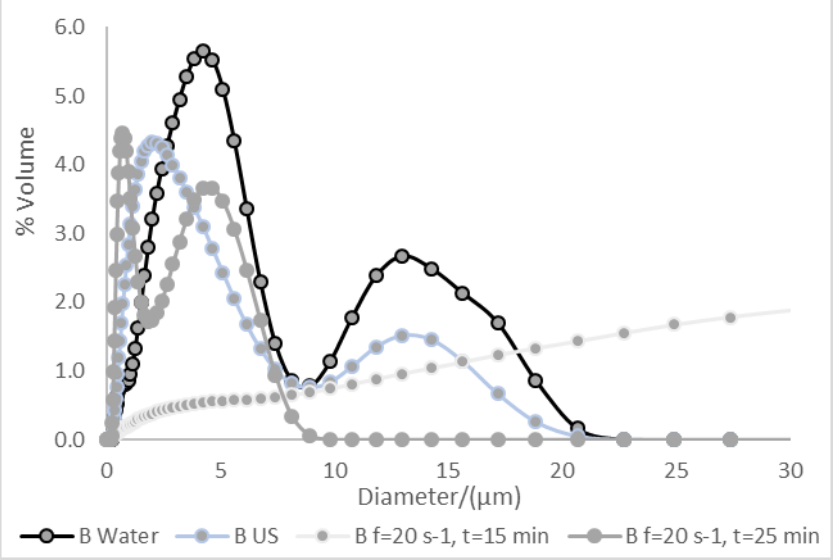

Appendix Figure 6: B particle size distribution

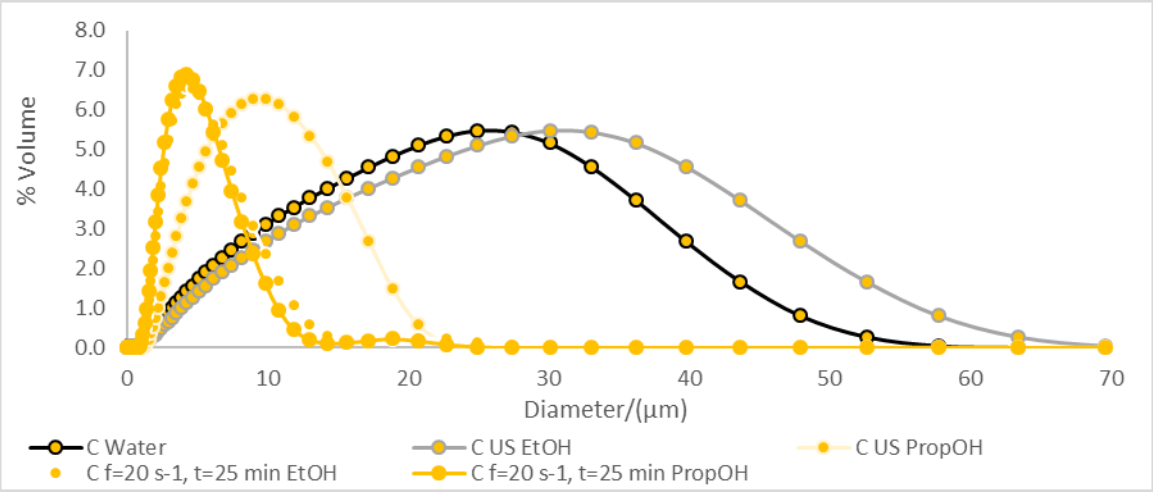

Appendix Figure 7: C particle size distribution including propanol (PropOH) suspensions

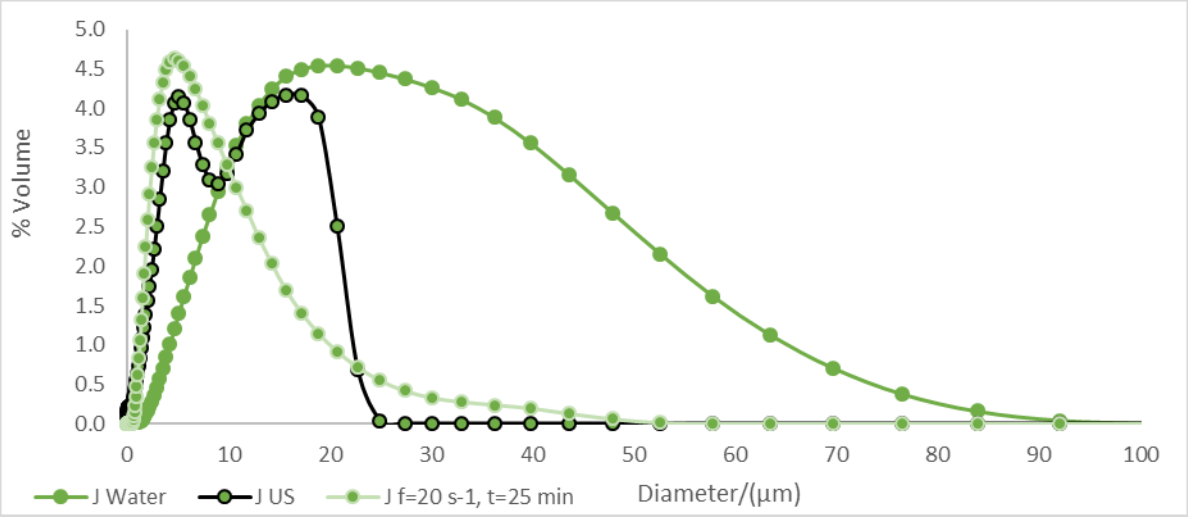

Appendix Figure 8: J particle size distribution

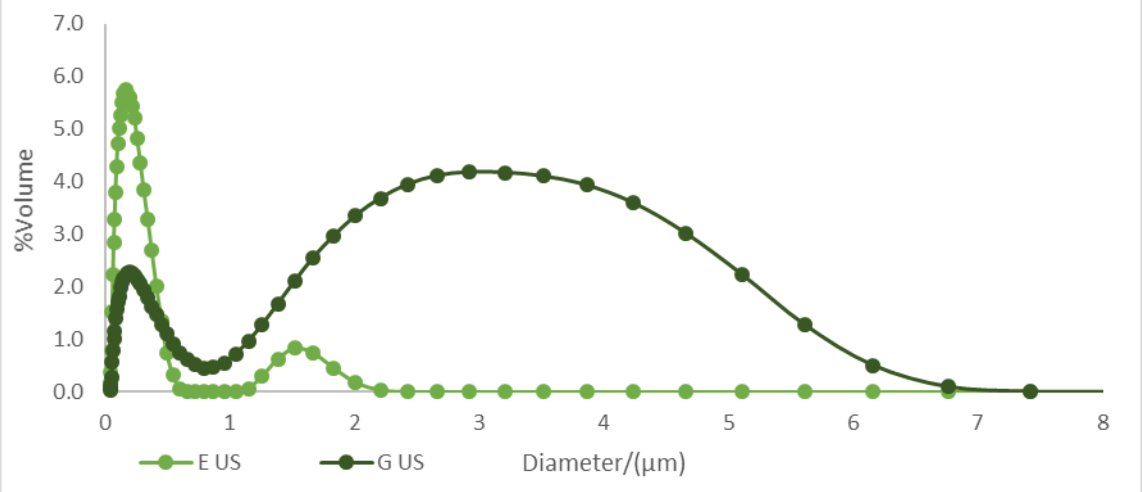

Appendix Figure 9: E and G particle distribution

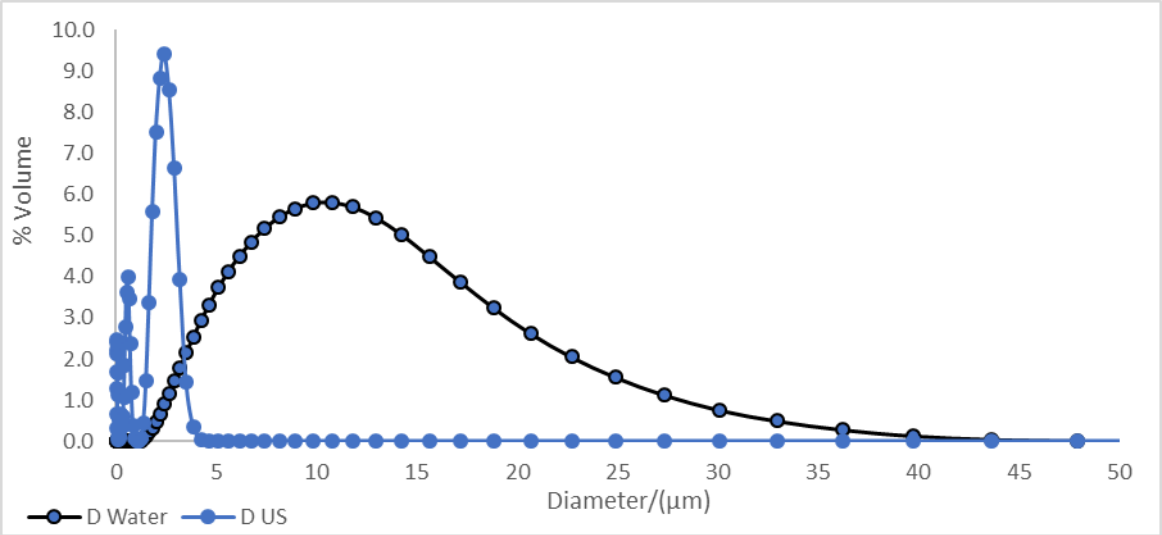

Appendix Figure 10: D particle size distribution

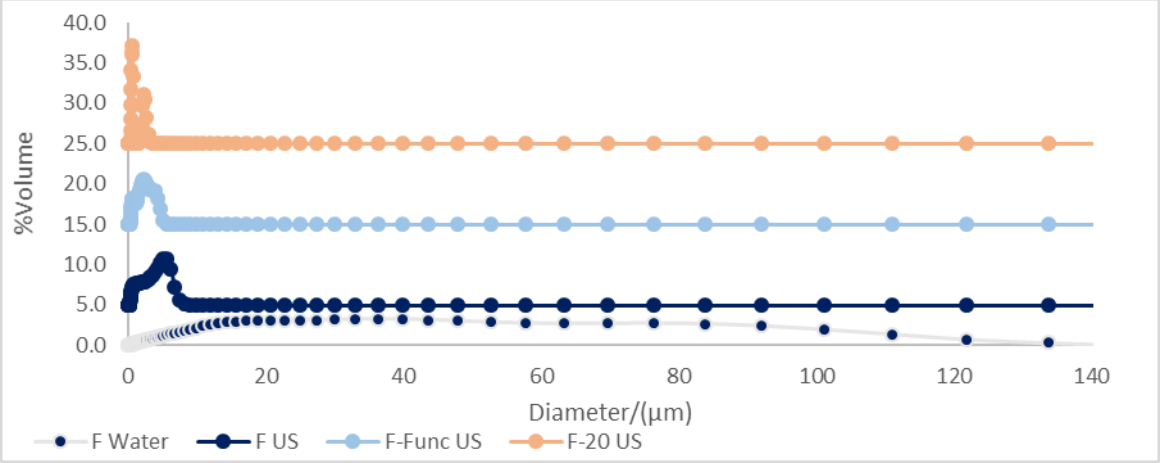

Appendix Figure 11: F samples particle size distribution

Appendix 5 Catalysts Textural Characterization: N_2 absorption at -196 °C

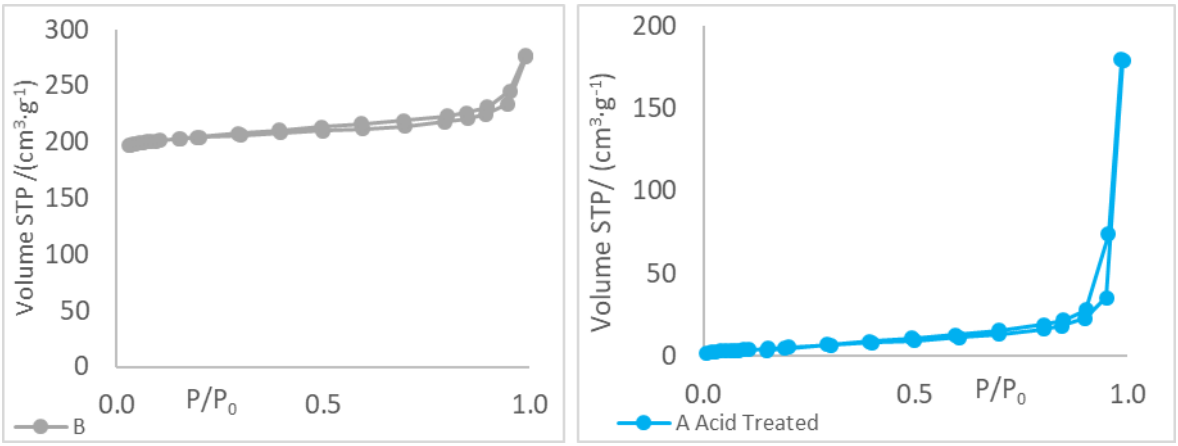

Appendix Figure 12: B and A Acid Treated isotherms

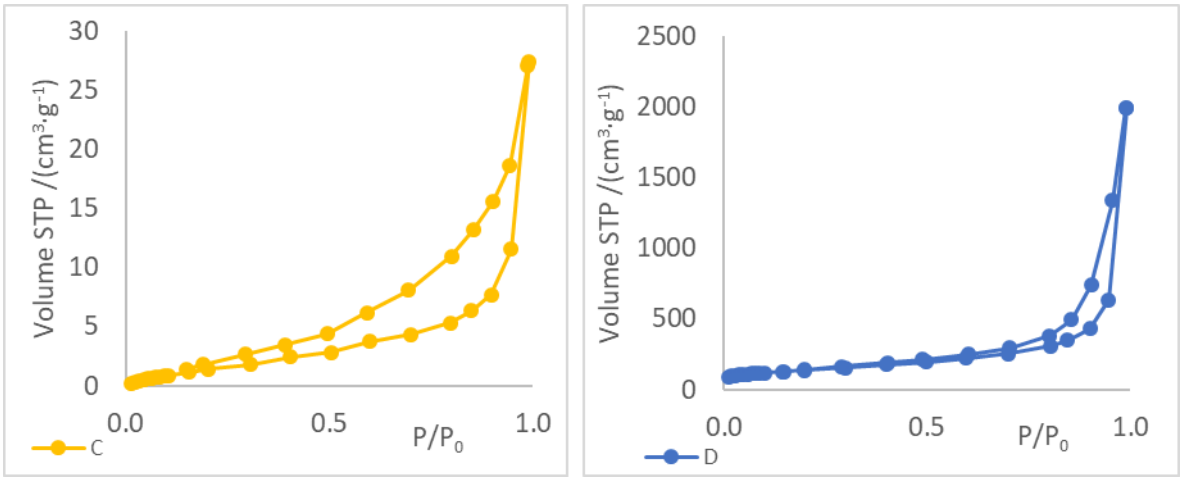

Appendix Figure 13: C and D isotherms

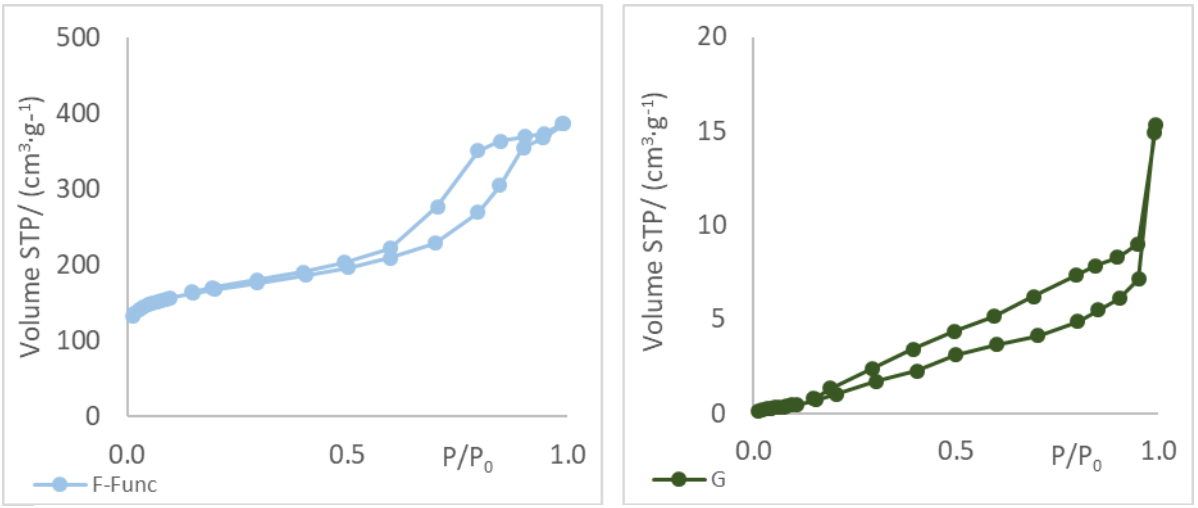

Appendix Figure 14: F-Func and G isotherms

Appendix 6 Catalysts Thermogravimetry Analysis

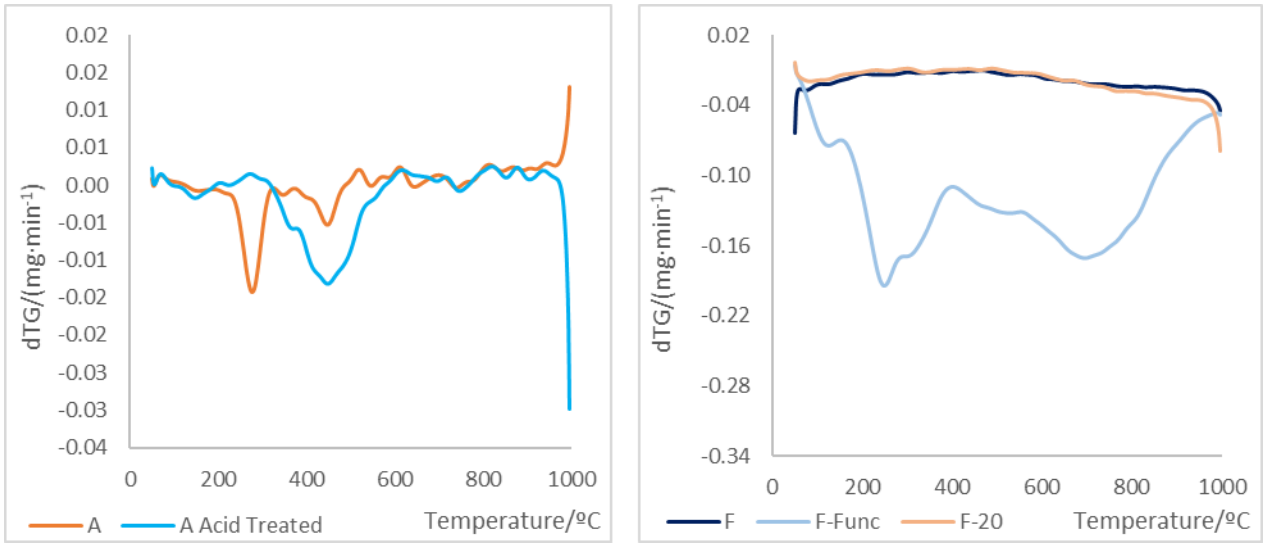

Appendix Figure 15: A and F non treated and treated samples 1st derivatives

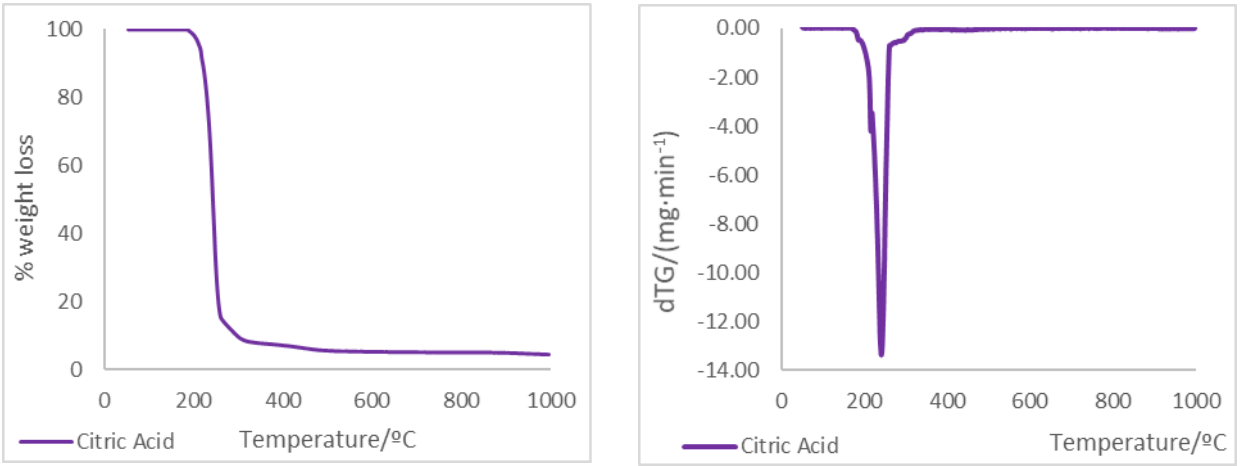

Appendix Figure 16: Citric Acid thermogravimetric analysis

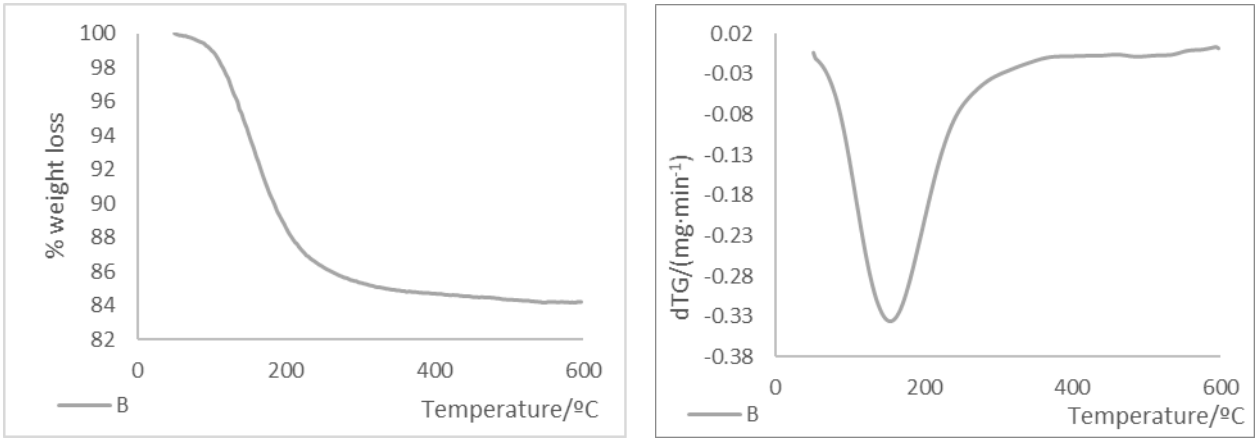

Appendix Figure 17: B thermogravimetric analysis

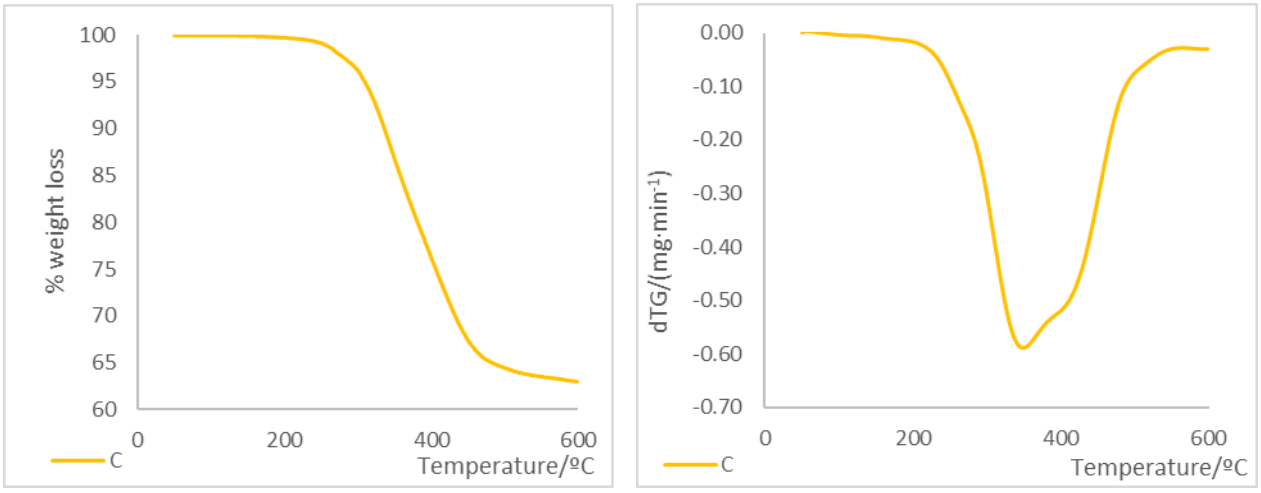

Appendix Figure 18: C thermogravimetric analysis

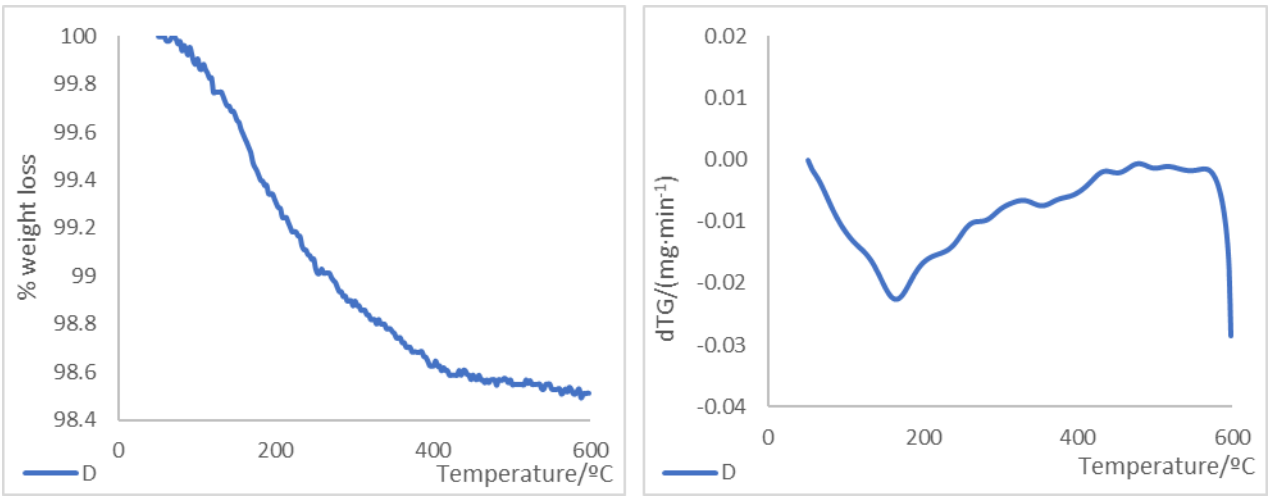

Appendix Figure 19: D thermogravimetric analysis

Appendix 7 Hydrolysis Control Test

Appendix Table 2: Verification of thermogravimetric analysis reproducibility

Control 0 h	Control 1	Control 2	Control 3	Average ± s.d.
T_{onset} (°C)	356	363	361	360 ± 2.8
$T_{5\,\%}$ (°C)	339	351	348	346 ± 5.1
$T_{10\,\%}$(°C)	351	361	358	357 ± 3.9
T_{peak} (°C)	386	388	388	387 ± 0.8
Total Weight Loss (%)	97	97	97	97 ± 0.3

Appendix Table 3: Thermogravimetric analysis of the hydrolysis test to verify the changes within positions 1, 2, 4: 240 h

168 h	1	2	4	Average ± s.d.
T_{onset} (°C)	357	359	356	358 ± 1.4
$T_{5\,\%}$ (°C)	335	338	331	334 ± 2.9
$T_{10\,\%}$(°C)	350	350	346	349 ± 2.1
T_{peak} (°C)	390	388	386	388 ± 1.8
Total Weight Loss (%)	98	99	98	98 ± 0.4

Appendix Table 4: Thermogravimetric analysis of the hydrolysis test to verify the changes within positions 1, 3, 5: 240 h

240 h	1	3	5	Average ± s.d.
T_{onset} (°C)	345	351	348	348 ± 2.2
$T_{5\,\%}$ (°C)	313	333	330	325 ± 8.6
$T_{10\,\%}$(°C)	331	343	340	338 ± 5.1
T_{peak} (°C)	378	378	373	376 ± 2.5
Total Weight Loss (%)	97	88	90	92 ± 3.8

Appendix Table 5: Thermogravimetric analysis of the hydrolysis test to verify the changes within positions 1 to 4: 312 h

312 h	1	2	3	4	Average ± s.d.
T_{onset} (°C)	343	350	351	350	351 ± 0.8
$T_{5\,\%}$ (°C)	321	323	311	316	313 ± 2.5
$T_{10\,\%}$(°C)	333	338	331	333	332 ± 1.3
T_{peak} (°C)	381	383	383	381	382 ± 1.3
Total Weight Loss (%)	97	97	99	98	98 ± 0.4

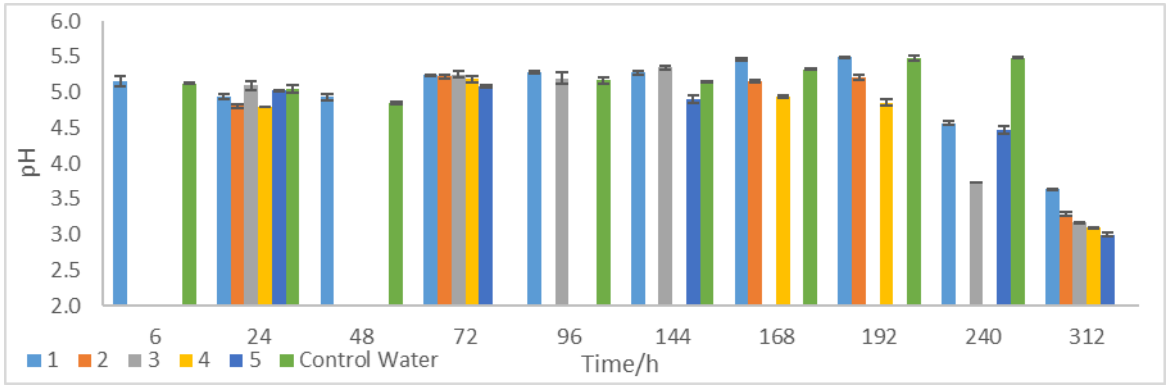

Appendix Figure 20: pH control hydrolysis test results

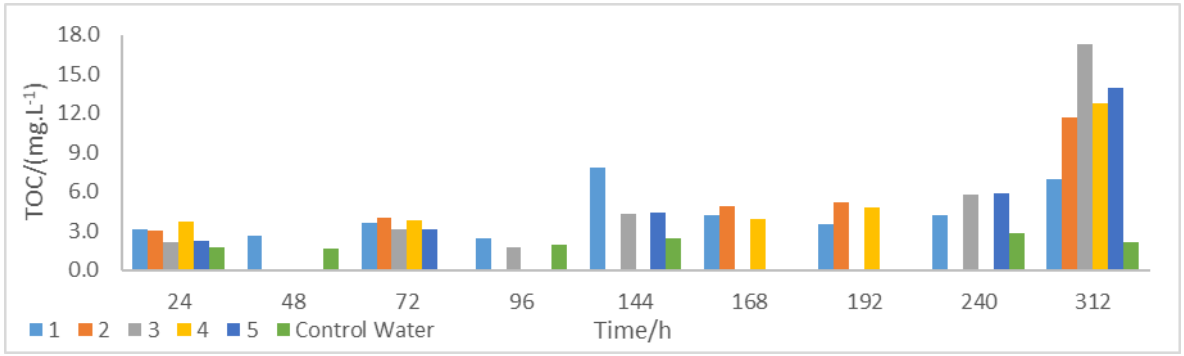

Appendix Figure 21: TOC control hydrolysis test results

Appendix 8 PLA Fibre Gel Permeation Chromatography Analysis

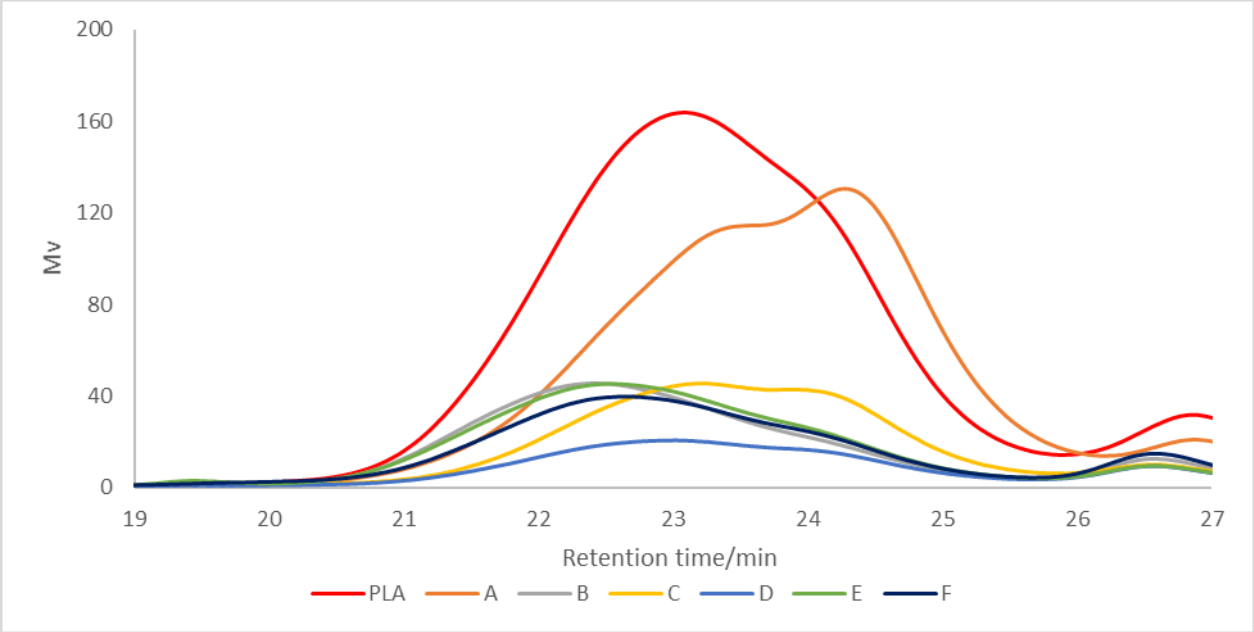

Appendix Figure 22: GPC analysis for the 1st batch after 240 h 70 °C hydrolysis

Appendix 9 Fibres Thermogravimetric Analysis

Appendix Table 6: Before hydrolysis thermogravimetric analysis

0 h	PLA	A	B	C	D	E	F	Polymer_A	Polymer_B	Process_Aid	G	F-Func	F-20
T_{onset} (°C)	360	298	351	351	359	355	361	355	357	357	355	361	362
$T_{5\,\%}$ (°C)	341	133	338	326	343	328	348	338	351	348	343	348	351
$T_{10\,\%}$ (°C)	356	273	346	343	353	348	358	350	356	356	353	358	361
T_{peak} (°C)	381	321	368	371	386	376	388	383	381	381	381	385	386
Δ to T_{peak} of PLA (%)	-	-15.8	-3.3	-2.6	1.3	-1.3	1.9	0.6	-0.1	-0.1	0.0	1.3	1.3
Δ to T_{peak} of 0 h (%)	99	100	97	97	96	97	94	96	95	96	95	97	96

Appendix Table 7: 70 ºC hydrolysis after 240 h

240 h 70 °C Hydrolysis	PLA	A	B	C	D	E	F	PLA 2nd	Polymer_A	Polymer_B	Process_Aid	G	F-Func	F-20
T_{onset} (°C)	349	299	335	355	329	363	351	349	348	318	314	330	358	359
$T_{5\,\%}$ (°C)	303	281	313	328	291	348	326	321	311	298	296	311	341	328
$T_{10\,\%}$ (°C)	331	293	326	343	308	361	341	336	331	308	308	321	353	346
T_{peak} (°C)	383	323	366	386	376	386	381	371	366	348	333	361	386	386
Δ to T_{peak} of PLA (%)	-	-15.7	-4.6	0.6	-2.0	0.6	-0.6	-3.3	-4.6	-9.1	-13.1	-5.9	0.6	0.6
Δ to T_{peak} of 0 h (%)	0.7	0.8	-0.7	4.0	-2.6	2.7	-1.9	-2.6	-4.5	-8.5	-12.4	-5.2	0.0	0.0
T_{onset} (°C)	99	95	94	94	98	94	92	95	96	95	87	93	92	99

Appendix Table 8: 40 ºC hydrolysis after 240 h

240 h 40 °C Hydrolysis	PLA	A	B	C	D	F-Func
T_{onset} (°C)	360	288	341	352	302	311
$T_{5\,\%}$ (°C)	341	263	313	346	298	296
$T_{10\,\%}$ (°C)	353	278	328	351	306	306
T_{peak} (°C)	378	311	358	368	326	331
Δ to T_{peak} of PLA (%)	-	-17.8	-5.3	-2.7	-13.9	-12.5
Δ to T_{peak} of 0 h (%)	-0.7	-3.1	-2.7	-0.7	-0.2	-14.2
T_{onset} (°C)	100	96	94	96	86	94

Appendix 10 Tensile tests

Appendix Table 9: Mechanical tests results of fibres with non-treatment applied and variation to the pristine fibre

Non treatment applied	den	Tenacity ± s.d. ($g \cdot den^{-1}$)	Δ (PLA) (%)	Elongation ± s.d. (%)	Δ (PLA) (%)
Pristine PLA	350	3.4 ± 0.2	-	22.9 ± 0.75	-
PLA+1 % A+0.25 % Process_Aid	340	2.6 ± 0.2	-24.9	26.9 ± 0.83	17.6
PLA+1 % B+0.25 % Process_Aid	340	2.8 ± 0.2	-17.9	22.9 ± 0.81	0.1
PLA+1 % C+0.25 % Process_Aid	390	3.0 ± 0.2	-12.1	28.4 ± 0.68	23.8
PLA+1 % D+0.25 % Process_Aid	410	2.8 ± 0.2	-17.7	25.0 ± 0.92	9.0
PLA+1 % E+0.25 % Process_Aid	380	3.3 ± 0.2	-5.7	25.0 ± 0.89	9.1
PLA+1 % F+0.25 % Process_Aid	390	2.8 ± 0.1	-18.2	23.8 ± 0.39	3.9
PLA+3 % Polymer_A +0.25 % Process_Aid	360	3.2 ± 0.5	-6.7	23.3 ± 1.79	1.9
PLA+3 % Polymer_B +0.25 % Process_Aid	360	3.4 ± 0.3	-2.0	24.1 ± 0.89	5.3
PLA+0.25 % Process_Aid	380	3.1 ± 0.8	-9.5	21.7 ± 3.12	-5.4
PLA+1 % G+0.25 % Process_Aid	380	3.1 ± 0.3	-11.5	24.4 ± 0.99	6.7
PLA+1 % F-Func+0.25 % Process_Aid	370	2.5 ± 0.1	-28.5	21.5 ± 0.40	-6.2
PLA+1 % F-20+0.25 % Process_Aid	390	2.4 ± 0.2	-31.7	19.4 ± 0.74	-15.2
PLA+1 % (A Acid Treated)+0.25 % Process_Aid	360	2.2 ± 0.2	-37.0	22.2 ± 0.65	-3.2

Appendix Table 10: Mechanical tests results of fibres after heat treatment and variations (Δ)

After heat treatment	Tenacity ± s.d. ($g \cdot den^{-1}$)	Δ (non treatment) (%)	Δ (PLA after heat treatment) (%)	Elongation ± s.d. (%)	Δ (non treatment) (%)	Δ (PLA after heat treatment) (%)
Pristine PLA	3.8 ± 0.1	10.6	-	27.4 ± 0.44	19.7	-
PLA+1 % A+0.25 % Process_Aid	2.7 ± 0.2	3.2	-29.9	27.4 ± 0.57	1.9	0.1
PLA+1 % B+0.25 % Process_Aid	3.0 ± 0.2	7.2	-20.4	24.2 ± 0.51	5.7	-11.7
PLA+1 % C+0.25 % Process_Aid	3.2 ± 0.3	5.9	-15.7	30.5 ± 1.11	7.5	11.2
PLA+1 % D+0.25 % Process_Aid	2.9 ± 0.1	0.9	-24.9	25.6 ± 0.52	2.5	-6.7
PLA+1 % E+0.25 % Process_Aid	3.7 ± 0.0	14.6	-2.2	28.6 ± 0.19	14.3	4.1
PLA+1 % F+0.25 % Process_Aid	2.9 ± 0.1	1.1	-25.2	24.9 ± 0.54	4.6	-9.2
PLA+3 % Polymer_A +0.25 % Process_Aid	3.7 ± 0.3	14.8	-3.1	27.7 ± 0.99	18.7	1.0
PLA+3 % Polymer_B +0.25 % Process_Aid	3.9 ± 0.1	15.0	2.0	28.9 ± 0.32	19.8	5.4
PLA+0.25 % Process_Aid	3.7 ± 0.2	18.5	-3.0	28.3 ± 0.88	30.6	3.2
PLA+1 % G+0.25 % Process_Aid	3.1 ± 0.1	1.6	-18.6	26.7 ± 0.70	9.1	-2.8
PLA+1 % F-Func+0.25 % Process_Aid	2.6 ± 0.0	3.9	-32.8	24.9 ± 0.21	15.9	-9.2
PLA+1 % F-20+0.25 % Process_Aid	2.5 ± 0.0	5.5	-34.8	25.2 ± 0.16	29.6	-8.2
PLA+1 % (A Acid Treated)+0.25 % Process_Aid	1.9 ± 0.3	-11.9	-49.8	20.7 ± 1.22	-6.6	-24.5

Appendix Table 11: Mechanical tests results of fibres after 240 h 40 ºC hydrolysis and variations (Δ)

240 h 40 ºC Hydrolysis	Tenacity ± s.d. ($g \cdot den^{-1}$)	Δ (non treatment) (%)	Δ (PLA after 40 ºC hydrolysis) (%)	Elongation ± s.d. (%)	Δ (non treatment) (%)	Δ (PLA after 40 ºC hydrolysis) (%)
Pristine PLA	3.2 ± 0.2	-6.4	-	28.3 ± 0.59	0.2	-
PLA+1 % A+0.25 % Process_Aid	2.1 ± 0.1	-18.2	-34.3	26.4 ± 0.53	-2.0	-6.7
PLA+1 % B+0.25 % Process_Aid	2.6 ± 0.2	-8.5	-19.7	23.7 ± 0.71	3.3	-16.2
PLA+1 % C+0.25 % Process_Aid	2.9 ± 0.1	-5.0	-10.7	32.4 ± 0.33	14.3	14.7
PLA+1 % D+0.25 % Process_Aid	2.6 ± 0.1	-7.5	-18.6	27.0 ± 0.45	-8.0	-4.6
PLA+1 % F-Func+0.25 % Process_Aid	2.5 ± 0.1	0.8	-22.9	24.3 ± 0.23	-1.0	-14.1